Low Generation Degradable Dendrimer Nanoclusters for Delivery of Anti-cancer Drug

Thesis submitted to University of Madeira in order to obtain the degree of Master in Nanochemistry and Nanomaterials

By Akudari Raja Shekar

Study performed under the supervision of Dr. Yulin Li and co-supervised by

Prof. João Rodrigues and Prof. Helena Tomás

Centro de Competência de Ciências Exatas e de Engenharia,

Centro de Química da Madeira,

Campus Universitário da Penteada, 9000-390 Funchal, Portugal

Outubro de 2014

DECLARATION

I hereby declare that this thesis is the result of my own work, is original and was written by me. I also declare that its reproduction and publication by Madeira University will not break any third party rights and that I have not previously (in its entirety or in part) submitted it elsewhere for obtaining any qualification or degree. Furthermore, I certify that all the sources of information used in the thesis were properly cited.

10/2014

ACKNOWLEDGEMENTS

I am grateful to everyone that directly or indirectly contributed to the execution of my project work, especially to my supervisor Dr. Yulin Li and to my co-supervisor Prof. Helena Tomás and Prof. João Rodrigues, for the collaboration and the guidance in my research and for providing the materials and facilities for the development of this project.

I also want to extend my sincere thanks to the chemistry lab assistants for providing me with all the equipment and chemicals whenever I needed and for helping me during my work.

My gratitude to the following Molecular Material Research Group (MMRG), members, Dina Maciel, Guoying Wong, Claudia Camacho, Dr. Carla Alves, Mara Goncalves, Rita Castro and Carla Miguel not only for their guidance during all my work, but also for their friendship. I want to thank Nilsa Oliveira, as whenever I needed to do NMR, she always offered me help.

I would like to thank also all members of Centro de Química da Madeira (CQM), for the friendship and support, not only in the lab, but also in the meetings and gatherings.

I acknowledge the University of Madeira and CQM for providing me the possibility to perform my master project.

Finally, I would like to acknowledge the Portuguese "Fundação para a Ciência e a Tecnologia" (FCT-IP) for funding through the CQM Strategic Project PEst-OE/QUI/UI0674/2013, the NMR Portuguese Network PTNMR-2013, and the Projects FCT-IP Project PTDC/CTM-NAN/116788/2010 and PTDC/CTM-NAN/112428/2009. FCT-IP is also acknowledged for the Science 2008 Programme (Y. Li).

During this master thesis, I learned chemical synthesis methods, and how to use several characterization instruments such as the NMR spectrometer, the Fourier transform infra-red (FTIR) spectrometer, the ultraviolent visible (UV-Vis) spectrometer, the Zetasizer, the fluorescence microscope, fluorescence spectrophotometer etc.. Moreover, I got acquainted with cell culture techniques (from recovering cells from liquid nitrogen to cytotoxicity tests of the modified dendrimer nanoclusters) for biological evaluation of drug loaded nanosystems.

Work presentations in Scientific Meetings in the scope of the Master Project:

Akudari Raja Shekar , Yulin Li, João Rodrigues, Helena Tomás. Low Generation Degradable Dendrimer Nanoclusters for Delivery of Anti-cancer Drug. Oral presentation in the 9th Materials Group Meeting of CQM. 31 January 2014; Funchal (Portugal).

ABSTRACT*:*

Although doxorubicin (DOX) has been widely investigated for treatment of different types of cancer, its poor cellular uptake and intracellular release still limit its further clinical applications (*1*). Due to their favourable characteristics, including the well-defined architecture, multivalency, and modifiable surface functionality, poly(amidoamine) (PAMAM) dendrimers have been extensively investigated for biomedical applications (*2*). However, most of the dendrimers are nondegradable, consequently resulting in high toxicity and uncontrollable drug release with limited release efficiency, which limits their further application in delivery of therapeutic agents (*3*).

Low generation dendrimers are less expensive, possess a low number of defects and are more biocompatible than those of high generation. In this work degradable dendrimer nanoclusters were prepared by crosslinking of low generation PAMAM dendrimers (Generation 3, G3) using *N, N'*- cystamine-bis-acrylamide (CBA) as a disulphide containing cross linker. The synthesized G3-CBA was then PEGylated using methoxyl poly(ethylene glycol) carboxylic acid (m-PEG-COOH) (MW 2000 g/mol) for further improvement of the colloidal stability, which can be also helpful for prolonging the circulation period as well as reducing their toxicity, immunogenicity and antigenicity.

The resulting G3-CBA-PEG dendrimers were characterised using Nuclear Magnetic Resonance (NMR), Fourier Transform Infra-Red Spectroscopy (FTIR), and Dynamic Light Scattering (DLS) to confirm the structure of G3-CBA and their PEGylated form (G3-CBA-PEG). UV-Visible Spectroscopy technique was also performed to study the encapsulation of drug in the synthesized dendrimer nanoclusters.

DOX, as a model drug was loaded into the resulting G3-CBA-PEG to obtain drug-loaded nanosystems (G3-CBA-PEG/DOX), which have been tested for anticancer drug delivery, concerning their drug release properties and anticancer cytotoxicity and cellular uptake through evaluation against CAL-72 cells (an osteosarcoma cell line). The results indicate that G3-CBA-PEG/DOX presented a pH and redox sensitive drug release in a sustainable way. The G3-CBA-PEG showed a reduced cytotoxicity than G3 dendrimers. G3-CBA-PEG/DOX presented a comparable anticancer cytotoxicity as compared with G3/DOX. The merits of the low generation PAMAM dendrimers, such as good cytocompatibility, sustained pH- and redox- dual cell responsive release properties, and improved anticancer activity, make them a promising platform for the delivery of other therapeutic agents beyond DOX.

Keywords: Dendrimers; nanoclusters; doxorubicin; drug delivery.

RESUMO:

A doxorrubicina (DOX) tem sido amplamente investigada para o tratamento de diferentes tipos de cancro. Contudo, a sua má internalização e libertação celular limitam ainda novas aplicações clínicas (*1*). Dadas as suas características favoráveis, onde se incluem a arquitectura bem definida, multivalência e possibilidade de modificação da superfície (funcionalização), os dendrímeros de poli(amidoamina) (PAMAM) têm sido amplamente investigados para aplicações biomédicas (*2*). No entanto, a maioria dos dendrímeros não são degradáveis, resultando numa alta toxicidade e libertação descontrolada do fármaco o que limita a sua eficiência de libertação e posterior aplicação na entrega de agentes terapêuticos (*3*).

Neste trabalho prepararam-se dendrímeros PAMAM biodegradáveis por reticulação de dendrímeros PAMAM de baixa geração (Geração 3, G3) usando cistaminabisacrilamida (CBA) como um agente de reticulação contendo dissulfureto. Estes dendrímeros são mais baratos, apresentam um baixo índice de defeitos e são mais biocompatíveis que os de alta geração.

O G3-CBA sintetizado foi posteriormente modificado com polietileno glicol (PEG) utilizando o *m*-PEG-COOH (M_W 2000) para camuflá-lo do sistema imunitário do hospedeiro ou para uma imunogenicidade reduzida e antigenicidade. A modificação com o PEG também ajuda a aumentar o tamanho hidrodinâmico da droga o que proporciona um aumento do tempo de circulação, reduzindo a depuração renal.

Os dendrímeros G3-CBA-PEG resultantes foram caracterizados por Ressonância Magnética Nuclear (RMN), Espectroscopia de Infra-vermelho com Transformada de Fourier (FTIR), Dispersão Dinâmica de Luz (DLS) e por espectroscopia de UV-Visível para confirmar a polimerização do G3-CBA, a modificação com o PEG do G3-CBA-PEG, para medir o tamanho hidrodinâmico do nano-cluster e para caracterizar e medir o encapsulamento de doxorrubicina em G3-CBA-PEG.

A DOX, como um fármaco modelo, foi encapsulada no G3-CBA-PEG para obter nanosistemas (G3-CBA-PEG/DOX). Estes foram posteriormente testados em células CAL-72 (linha celular de osteosarcoma) para entrega deste fármaco anticancerígeno, considerando as suas propriedades de libertação, citotoxicidade e internalização celular. O sistema G3-CBA-PEG/DOX revelou uma libertação controlada do fármaco que era dependente do pH e das condições de oxidação-redução. O G3-CBA-PEG exibiu uma citotoxicidade inferior

à dos dendrímeros G3 e o sistema G3-CBA-PEG/DOX apresentou uma citotoxicidade anticancerígena comparável à do G3/DOX. Os atributos dos dendrímeros PAMAM de baixa geração, a boa citocompatibilidade, a capacidade de reposta celular e a libertação do fármaco controlada e dependente do pH e das condições de oxidação-redução, e atividade anticancerígena melhorada, fazem deles uma promissora plataforma para entrega de outros agentes terapeuticos além da DOX.

Palavras-chave: Dendrímeros; nanoagregados; doxorrubicina; entrega de fármacos.

CONTENTS

LIST OF ACRONYMS

AA – Antibiotic and antimycotic

CBA –N, N'- Cystamine-bis-Acrylamide

DAPI – 4', 6-Diamidino-2-Phenylindole

DOX – Doxorubicin

DMEM – Dulbecco's Modified Eagle's Medium

DNA – Deoxyribonucleic acid

EDC – 1-ethyl-3-(3-dimethylaminopropyl)carbodiimide

EPR – Enhance Permeability and Retention

FDA – Food and Drug Administration

G3 – Generation 3

Glut – L-Glutamine

KBr – Potassium Bromide

mPEG – Methoxy Poly Ethylene Glycol

MRI – Magnetic Resonance Imaging

MWCO – Molecular Weight Cut-Off

NMR – Nuclear Magnetic Resonance

NPs – Nanoparticles

PAMAM – Poly(amidoamine)

PBS – Phosphate Buffered Saline

PEG – Polyethylene Glycol

POPAM –Poly(propyleneamine)

PPI – Poly(propyleneimine)

TGA - Thioglycolic Acid

LIST OF FIGURES

LIST OF TABLES

CHAPTER 1 – INTRODUCTION

CHAPTER 1 – INTRODUCTION

1.1 Introduction to dendrimers

Dendrimers are branched three-dimensional molecules which possess uncustomary molecular architectures and unique properties that make these alluring materials for the advancement of nanomedicines (*4*).

Dendrimers are mainly composed of three distinguishable domains (Figure 1):

(i) A single atom or an atomic group having at least two similar chemical functions as a central core

(ii) Branches evolving from the core, integrated of repeat units with at least one branch junction, whose iteration is organized in a geometrical progression which finally results in a series of deviated concentric layers called generations, and

(iii) Many terminal functional groups, which are usually positioned on the periphery of the macromolecule, which play an important role in the physico-chemical properties.

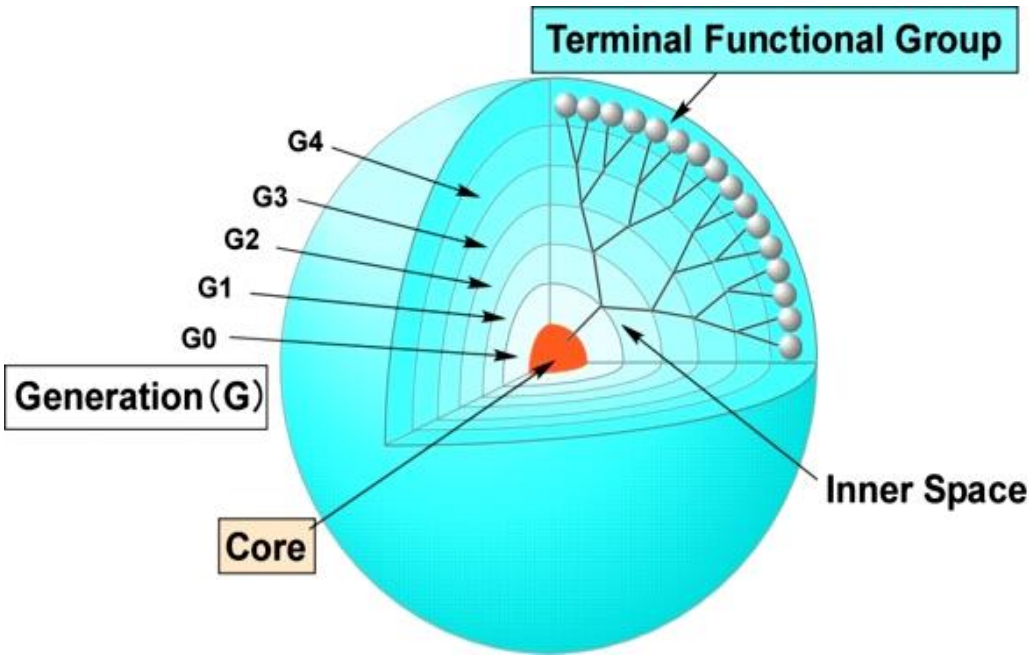

Figure 1 – Structure of dendrimer (*5*).

1.2 Approaches to synthesize dendrimers

Dendrimers are generally large molecules with high molecular weight, regular and massively branched structures; these macromolecules are multivalent and their dimensions resembles to those of small proteins. Synthetically these high molecular weight and well organised structures are generally synthesized via a cascade synthesis using an iterative sequence of reaction steps.

Dendrimers can be synthesized in each of these portions to have different functionality to control properties such as thermal stability, solubility, and for attachment of molecules for desired applications. Typical properties, such as the size and shape of the dendrimers as a function of generation, monomer distribution, solvent accessible surface area, and distribution of terminal groups are some of the critical aspects needed to be considered for some applications of dendrimers (*6*).

Generally, there are two synthetic strategies commonly used for development of dendrimers with different compositions and/or surface termini (*7-14*).

I. Divergent manner
II. Convergent manner

1.2.1 Divergent dendrimer synthesis

The divergent method was pioneered by Tomalia et al. (*15*). The synthesis of dendrimers is assembled from a multifunctional core building block, which is further extended outward radially by a series of reactions (Activation and Coupling), commonly by Michael reactions. Each reaction step must be handled very carefully and must be driven to full completion in order to avoid imperfections in the dendrimer structure. These imperfections can cause trailing generations (the phenomenon of having branches at different lengths and sizes) (*16*).

The synthesis of dendrimers takes by a stepwise layer-by-layer modification (Activation and Coupling) which starts from the core and eventually builds the molecule towards the periphery using two basic chemical manoeuvrings (*17*).

Firstly, the building blocks (branches) are coupled to the central core of the dendrimer which is the initiative of building the dendrimer structure. After that, the surface-group functionalities of the attached building blocks are modified (activated) for further growth. Higher generations of dendrimers can be prepared by repeating the reaction steps (*18*). The step by step reaction of the divergent synthesis of dendrimers is shown in Figure 2.

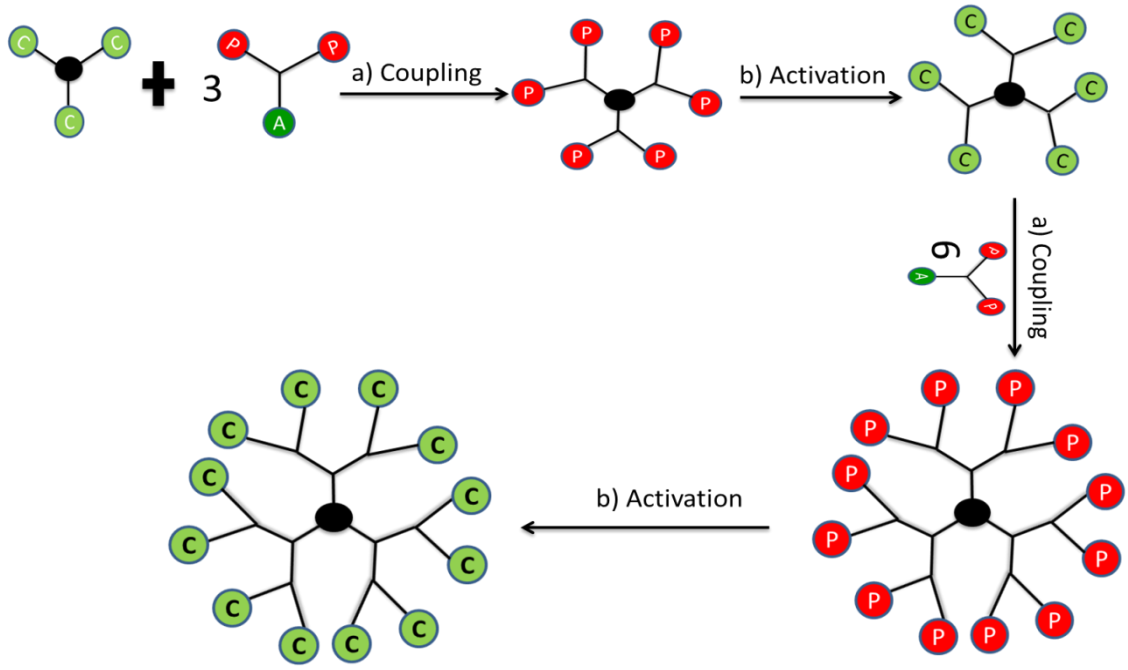

Figure 2 – Divergent synthesis of dendrimers. A= active unprotected functional group, P= protected, inactive (protective group) functionality, ● = core of the dendrimer, C= coupling group. Activation and Coupling are two repetitive steps contributing to the generation of Dendrimers (*21*).

1.2.1.1 Advantages of divergent synthesis

- Divergent synthesis is generally simple and controllable.
- Dendrimers with high molecular weight can be attained with a possibility of automation of the repetitive reaction steps.
- This method is highly recommended and normally used in the commercial production of Poly(amidoamine) PAMAM dendrimers (*19*).

1.2.1.2 Disadvantages of divergent synthesis

- Steric effects play an important role in the synthesis of high generation dendrimers as they can cause trailing generations.
- Impurities can have a greater impact on the functionality and symmetry of the dendrimer.
- The relative size difference between imperfect and perfect dendrimers is very small; hence purification and separation of dendrimers are very difficult (*20*).

1.2.2 Convergent dendrimer synthesis

The convergent strategy was first developed by Fréchet and Hawker in their synthesis of polybenzylether containing dendrimers with highly monodispersed dendrimer structures (*21*).

To circumvent the increasingly low reactivity accomplished during stepwise divergent synthesis, segment coupling strategies were applied to synthesise large oligopeptides of solid-phase. With the advancement of this new approach in peptide synthesis, one more step further was taken towards pure chemical synthesis of high molecular weights. This strategy of segmental coupling or convergent strategy was handy for the creation of dendritic macromolecular structures (*22*).

In contrast to the divergent method, the convergent method assembles a dendrimer from the periphery and inwards towards the core (outside inwards), by mostly “one to one” coupling of monomers therefore fabricating dendritic branches, dendrons, of increasing size as the synthesis process advances.

The final part of the convergent synthesis finishes up at the central core, where two or more dendritic segments (dendrons) will be joined together to form the dendrimer; the convergent strategy thus commonly has an inverse propagation correlated to the divergent strategy. The reaction steps involved in the convergent synthesis is shown below (Figure 3).

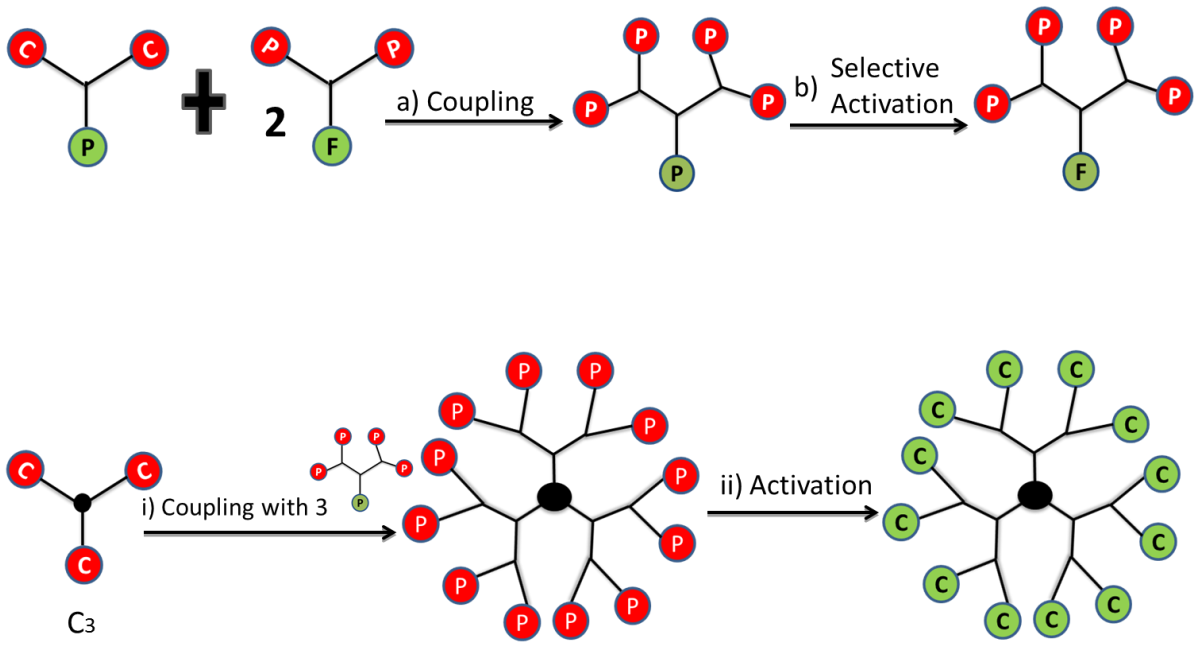

Figure 3 – Convergent synthesis of dendrimers. F= functional group, P= protective group, C= coupling group ● = core of the dendrimer. Reaction steps a) coupling and b) selective activation can be repeated until all segment-shaped dendrons of desired generation reacts with an oligo functional core module (C_3) to form the higher generation (*21*).

1.2.2.1 Advantages of convergent synthesis

- The number of reactive sites during the propagation process remains minimal leading to faster reaction rates and maximum yields.
- The most important advantage of this method is the large "molecular difference" between the reactant molecule and the product, which can facilitate the purification of the reactants from the product.
- Asymmetric dendrimers can be synthesised by coupling different segments together to obtain dendrimers with heterogeneous morphologies using convergent synthesis.

- Several “active sites” can be incorporated in one dendrimer to synthesize heterogeneous dendrimers with multifunctional molecular structures (*23*).

1.2.2.2 Disadvantages of convergent synthesis

- Only low generation dendrimers can be produced generally by this method due to the steric hindrance which limits the dimensions of the dendrimer growth during the reaction of dendrons at the periphery.
- As the generation of dendrimer increases, the reactive groups are densely covered at the focal point of the dendrons, and the attachment of the segmented units to the core-fragment becomes difficult (*24*).

1.2.3 Other synthetic methods for the synthesis of dendrimers

There are several other methods which are commonly used in the synthesis of dendrimers, they are (*10-14, 25-26*):

1) Click chemistry
2) Orthogonal synthesis
3) Double stage convergent method
4) Double exponential method
5) Hyper-monomer method
6) Solid phase synthesis
7) Co-ordination chemical synthesis
8) Supramolecular assembly.

These methods are not recommended for the production of dendrimers on a commercial scale but can be practised in laboratories and research institutions.

1.3 Physico-chemical properties of dendrimers

Dendrimers are monodispersed macromolecules. The key properties of dendrimers include circumscribed architecture, globular shape, low polydispersity index, and a high ratio of multivalent surface moieties to molecular volume which determines these nanoscaled materials highly fascinating for the evolution of synthetic (non-viral) vectors for therapeutic nucleic acids (*27-29*).

Unlike linear polymers, dendrimers show some significant improved physical and chemical properties because of their unique molecular structure. The presence of a large number of terminal groups is responsible for high reactivity, miscibility and for higher solubility. The solubility of the dendrimers is strongly influenced by the nature of terminal groups. Dendrimers which have hydrophilic terminal groups are soluble in polar solvents, while dendrimers terminated in hydrophobic groups are soluble in non-polar solvents (*30*).

Because of their unique globular shape and presence of internal cavities, dendrimers possess unique properties such as encapsulation of the guest molecules in their macromolecule interior (*31-33*). This unique property has opened a new way to encapsulate drugs, genes, proteins and other chemotherapeutics which are recently being used in numerous clinical applications.

"Cationic" dendrimers (e.g., amine terminated PAMAM and poly(propyleneimine) (PPI) dendrimers that form cationic groups at low pH) are generally haemolytic and cytotoxic. Their toxicity is generation-dependent and increases with the number of surface groups (*34*). While "Anionic" dendrimers, bearing a carboxylate surface group, are not cytotoxic over a broad concentration range (*35*). These biological properties play a crucial role in using dendrimers in biomedical applications.

In solution, linear polymer chains forms flexible coils; in contrary, dendrimers exist as a tightly packed ball (*30*). The viscosity of the dendrimer solutions is significantly lower than linear polymers (*31*). The intrinsic viscosity reaches maximum at generation 4 and then it begins to decrease when the molecular mass of dendrimers increases (*28*). Such behaviour is in contrast with linear polymers. For classical polymers when the molecular mass is increased the intrinsic viscosity increases continuously.

The properties of the dendrimers are also influenced by the functional groups present on the periphery. However, dendrimers with internal functionality were also reported (*37-39*).

Moreover, it is easier to make dendrimers water soluble, by functionalizing their terminal groups with hydrophilic groups or charged species. Other desirable and controllable properties of dendrimers include crystallinity, and chirality (*40*).

Numerous researches are being carried out to investigate the physico-chemical properties of dendrimers applying chemical analytical techniques and computer simulations. In order to optimise the computer models to deliver a prudent picture, comparative studies are being carried out between predictions based theoretical calculations and experimental results by chemical analysis (*41-42*).

Additionally, dendrimer chemistry is very alterable thus promoting broad range synthesis of various molecules with different functionality.

The two most important dendrimers which are used commonly are (*7, 43- 44*)

1) PAMAM
2) PPI.

These dendrimers have been produced industrially and are commercially available up to 10 generations.

1.4 PAMAM dendrimers

PAMAM dendrimers consist of polyamide branches with tertiary amines as focal points. After the initial report by Tomalia and co-workers (*45-46*) in the mid-1980s, PAMAM dendrimers have found numerous applications, ranging from gene therapy to molecular encapsulation and drug delivery, from micelle mimics as decontaminating agents to building blocks for nanostructures (*8*) and also provide many pharmaceutical, medicinal and clinical applications.

PAMAM dendrimers (Figure 4) are commercially available from Dendritech Inc. laboratories, usually as methanol solutions up to 10 generations, having terminal or surface amino groups (NH_3) (full generations) or carboxylic acid groups (COOH) (half-generations). Starburst dendrimers are applied as a trademark name for a sub-class of PAMAM dendrimers based on a tris-aminoethylene-imine core. This class of dendrimers are generally known with the abbreviation PAMAM. Fréchet-type dendrimers are a more recent type of dendrimer.

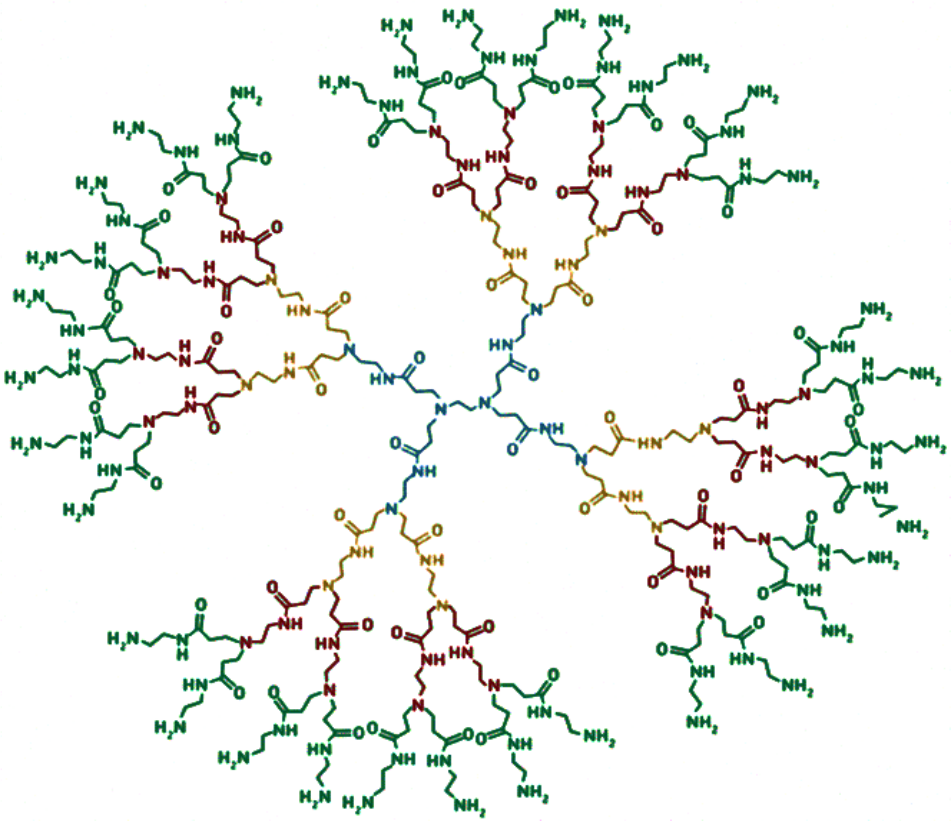

Figure 4 – Chemical structure of amino-terminated G3-PAMAM dendrimer (*47*)

PAMAM dendrimers are the most extensively studied macromolecules with spheroidal or an ellipsoidal shape. Due to the distinct synthesis process, PAMAM dendrimers have many interesting properties, which differentiate these macromolecules from classical linear polymers. Moreover, PAMAM dendrimers possess many functional peripheral groups and empty internal cavities, which play a most important role in increasing the solubility and attaining a high reactivity. The special structure and the more number of surface amino groups (NH_2) in PAMAM dendrimers may be expected to have numerous potential applications in increasing the solubility of the low aqueous solubility drugs or as delivery systems for bioactive reagents.

The unique synthesis of these dendrimers in a stepwise manner from monomer units allows the refined control over the dimensions, polarity, flexibility, size, solubility, shape, density and placement of different functional groups by choosing these building units and functional group chemistry. As a result, they have the combination of typical characteristics of small organic molecules and polymers that result in special physico-chemical properties.

Accordingly, PAMAM dendrimers have captivated increasing attention for their applications in many fields including drug delivery, gene delivery, etc (*46, 48*).

1.4.1 pH effect on PAMAM dendrimers

Amino-terminated PAMAM dendrimers have basic surface groups as well as a basic interior. At pH 7.4, most of the primary amines are protonated, and by pH 4.0 all of the tertiary amines are also protonated (*49*). Low pH commonly leads to extended conformations due to electrostatic repulsions between ammonium groups. At pH≤ 4 the interior is hollow as a result of repulsion between the tertiary amine groups in the interior and the positively charged amine groups on the surface. At pH≥ 10 the charge of the molecule becomes neutral, as the repulsive forces between the surface groups and the interior groups are very low and hence it contracts forming a spherical structure. Under physiological conditions (pH 7.4), the formation of strong hydrogen bonds between the surface amine groups (positively charged) and neutral or uncharged tertiary amines on the branches back-folding of the dendrimers occurs. Therefore, the PAMAM dendrimers indicate different properties under different pH values, which can be used for fabrication of pH sensitive platforms for therapeutic delivery systems (*50-51*).

1.5 Biomedical applications of dendrimers

Dendrimers are the most promising macromolecular structures which are being extensively studied in the recent years. Their globular structure and the desirable properties of the dendrimers made extensive progress in the field of life science. Dendrimers are considered promising structures in many clinical applications (52-*53*). The merits of dendrimers endow them with a variety of biomedical applications, such as drug delivery (*54-56*), gene transfection (*57-59*), magnetic resonance imaging (MRI) (*60-66*), bio-sensors (*67-68*), nano-scaffolds (*69-72*), therapeutics (drug and gene delivery) (*73-75*), nano drugs (*76-78*), diagnostics, etc..

Dendrimers as drug delivery systems are now creating opportunities for the studies in formulating efficient systems with drug stability and effective drug delivery to the targeted

sites. Some of the advantages of using dendrimers as drug delivery systems include a controlled release of the drug in the circulatory system (*79*), the accumulation of nanoparticles (NPs) at the target sites, protecting the drug form the external environment, reducing the unwanted side effects of the therapeutic agents (*80*). Recent research also shows that modifying the surface groups of the dendrimers can also affect the cytotoxicity and degradability of the dendrimers.

1.6 Dendrimers as drug delivery systems

Dendrimers often have been used as vehicles for drug delivery. Encapsulation of anti-cancer drugs (cisplatin and doxorubicin (DOX)) within PAMAM dendrimers showed sustainable drug release, reduced toxicity and improved drug accumulation in tumour cells/tissues when compared with the free drugs (*81*).

The three important reasons that justify the use of dendrimers for drug delivery are (*82- 84*):

i. Dendrimers are large structures with many terminal groups which can be modified with different substances that are capable of targeting receptor sites on cells.

ii. Formulation of many insoluble free drugs with dendrimers could enhance the solubility and thus increase the bioavailability.

iii. Dendrimers have large structures that exceed renal clearance and are not filtered out by the kidneys. Furthermore, the nanometric size may induce the Enhanced Permeability and Retention (EPR) effect.

Considering the above mentioned reasons which make the dendrimers more suitable for drug delivery, five different types of interactions are generally practiced for the encapsulation of drugs in dendrimers, which are shown in the Figure 5.

i. Synthesis of dendrimer prodrugs by covalently attaching the drug to the periphery of the dendrimer or by cleavable bond (case A and B).

ii. The drug is interacted non-covalently with the internal structure or to the outer functional groups (case C and D).

iii. Encapsulating the drug through the formation of a dendrimer-drug supramolecular assembly in which the dendrimer acts as a kind of macromolecular micelle (case E and F) (*85-86*).

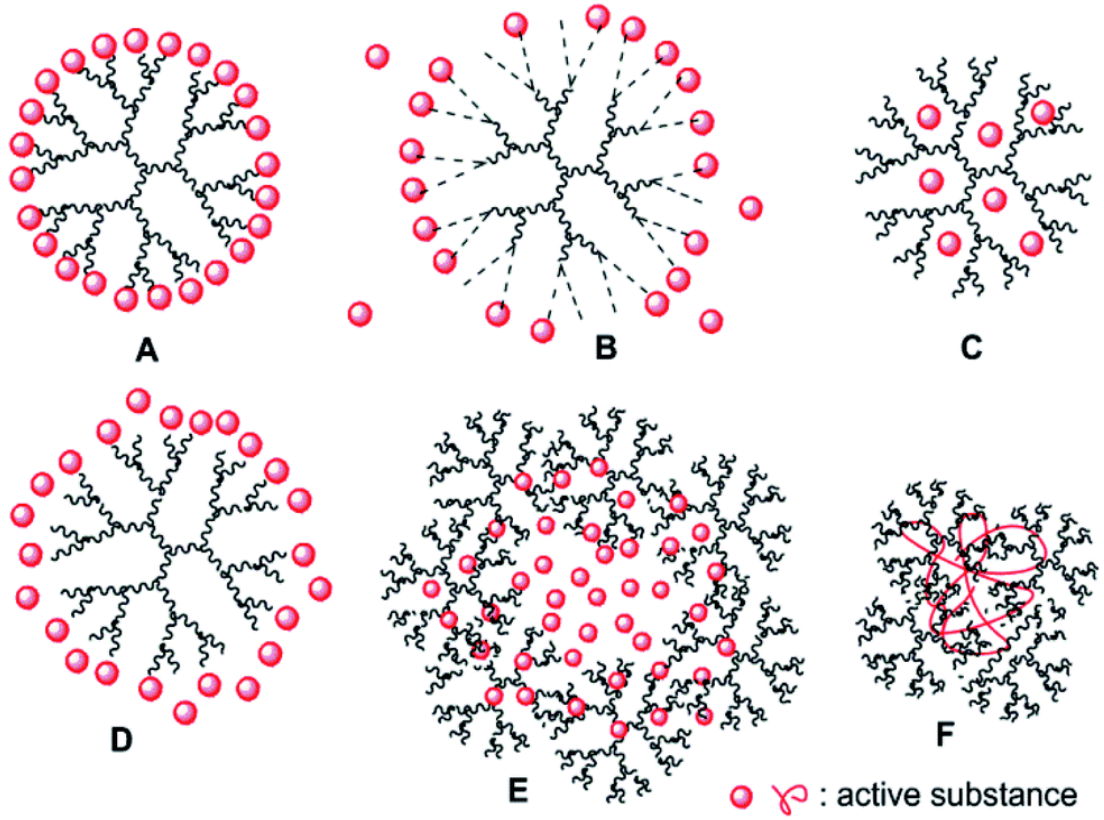

Figure 5 – Schematic representation of types of formulations for encapsulation of drug in dendrimers. Covalent attachment of the drug (case A and B); Non-covalent attachment of the drug (case C and D); Dendrimer drug-based supramolecular assembly (case E and F) (*87*).

Dendrimers are being widely studied for the controlled drug release, increased encapsulation of drugs, cellular uptake and for the increased retention time in the circulatory system. The encapsulation of the drug normally increases with the increase in the generation of the dendrimers, but due to cytotoxic effects of the higher generation dendrimers, generation 3-5 are considered as effective drug release systems (*88*).

1.6.1 Targeted drug delivery

Many anticancer drugs are available in the markets which are effective in killing the tumour cells, but due to their cytotoxic properties most of them are not being used in clinical applications. Numerous targeted drug delivery systems have been introduced and are being developed to optimize regenerative techniques. This targeted drug delivery system is based on an approach that is capable of delivering a certain amount of a therapeutic agent/drug for an extended period of time to a targeted tumour within the body. This method helps in maintaining the tissue drug levels and required plasma in the body, hence reducing cytotoxicity to the normal tissues (*89*).

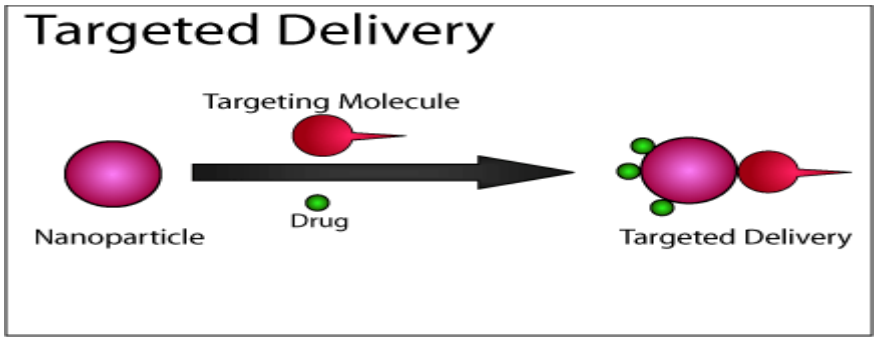

Figure 6 – Approach to design targeted drug delivery systems (*90*).

To design a system for targeted drug delivery requires plenty of effort and an excellent knowledge about the physiochemical activities occurring in the body. Ideal targeting drug delivery systems should present the following ideal characteristics (*91-92*):

a) They should be non-toxic and non-immunogenic,

b) They must present sufficient stable circulation period,

c) Drug release from the system into the target should not affect the drug action or its properties,

d) The systems must be degradable after the drug is released and should be eliminated from the body without causing any long term side effects to the normal cells,

e) Drug release should be controllable.

Targeted drug delivery systems are more effective than the classical drug delivery methods as they specifically target the tumour cells without interacting with the normal cells in the body. There are several kinds of strategies to direct the system to the tumour cells/tissues. In general two types of strategies can be followed

1) Active drug delivery system can be described as the system carrying the drug binds with the targeting molecules (proteins/folic acid) which have receptors for the targeted cells, which induce direct cellular uptake. This type of approach is also called as receptor mediated cellular uptake (*93*).

2) Passive drug delivery is based on the EPR effect. In order to grow rapidly the tumour cells must stimulate the production of blood vessels and other growth factors. To accumulate in the tumour, cells tend to take advantage of the increased permeability of the cancer blood vessels to take up the particles during circulation in the blood. As a result of this reaction the drug entrapped in the system can be released into the cells (*94*).

1.7 Degradable dendrimers using cross link molecules for drug and gene delivery

Degradable or cleavable dendritic structures (including dendrimers and hyper-branched polymers) have been unveiled for various applications, such as drug and gene delivery (*95*), molecular imprinting (*96*), generation of materials with microcavities (*97*) and release of fragrances and flavors (*98*) in which these structures function as a "covalent reservoir" (*99*).

Crosslinking is the most important concept in polymer chemistry and is extensively used in the fabrication of different materials for many applications. Due to the advancement in technology and research by the researchers, the crosslinking methodology has been developing rapidly. Cross linkages are not only used to link one polymer chain to another, but are also used to link other various chemical moieties together. A variety of crosslinking agents have been introduced in the recent years, such as acrylates (*100-101*), esters (*102-103*), olefins, organosilicons (*104-106*) to dendrimers, which have broad applications in the field of science. Cross linkage helps in easy dissolution in water and provides degradation of chemical species linked to them. Cross link chemistry is very reliable and hasfound many applications in drug and/or gene delivery.

Recent studies have shown that the degradability of dendrimers is enhanced when a disulphide cross link is used. The rapid cleavage of the disulphide linkages in the intracellular reductive environment (containing 0.1–10 mM glutathione) is biologically relevant to induce fast dissociation and efficient release of drugs and DNA. These studies also show that the degradability and release rates were lower at 20-40% of disulphide content, but were higher when more than 60% of the disulphide cross linked molecules were used. The disulphide content in these cross linked molecules also influence the transfection efficiency and cell viability. When more increments of disulphide content are added (more than 85 %), the formed materials have only marginal effects on the transfection efficiency and degradability (*107*).

1.8 PEGylation

In order to increase the possibility of nanomedicines to be accumulated around the tumour tissues, circulation time needs to be prolonged. Poly(ethylene-glycol) (PEG) is nontoxic, non-immunogenic, non-antigenic, and highly soluble in water and has been approved by the Food and Drug Administration (FDA) for human oral, intravenous and dermal pharmaceutical applications (*108*). Therefore, PEG has a crucial role in drug delivery and in designing the drug delivery systems. PEGylation through which PEG polymer chains are attached to another molecule by means of covalent bond is one of the most popular methods to achieve this purpose.

PEG is able to act as a protective coating constituent for drug delivery nanosystems (*109-110*), and has also contributed to the similar protection as a covalently bond conjugate to other drug molecules (*111*) and proteins (*112*). PEG is thus soluble in a wide variety of solvents (both non-polar and polar solvents) (*113*). Due to its important characteristics as a protective layer, PEG is often used to enhance the aqueous solubility or dissolution characteristics of hydrophobic drug molecules (*114-116*).

1.8.1 PEGylation strategies

PEGylation is typically an additional step, implemented at the end of an already existing process for the production of a given dendrimer. Several strategies have been proposed by many authors. There are different PEGylation strategies: site specific mono PEGylation is a generally practised technique in which highly reproducible products with maximum activity are produced. PEG also has an advantage of delivering the systems invisible to the liver, blood and splenic macrophages promoting retention in the diseased organ or blood. These types of carriers can act as a suitable platform in treating cancer by long circulatory lifetime of particles and by entrapment in the leaky vasculature of tumour (*117*). Alkylation is a technique which maintains the positive charge of the former amino group because of the formation of the secondary amine, or acylation, followed by loss of charge (*118,119*). The other PEGylation techniques include non-specific PEGylation, non-covalent PEGylation etc.

PEGylated dendrimers are generally biocompatible and show increased solubility when compared with the free molecules. These molecules provide complete packing for the drug and protect from different environments (pH conditions) and show a sustainable release (*120*). Various materials like multiple drugs, imaging agents, and DNA can be introduced as the PEGylated dendrimers provides more space (Figure 7).

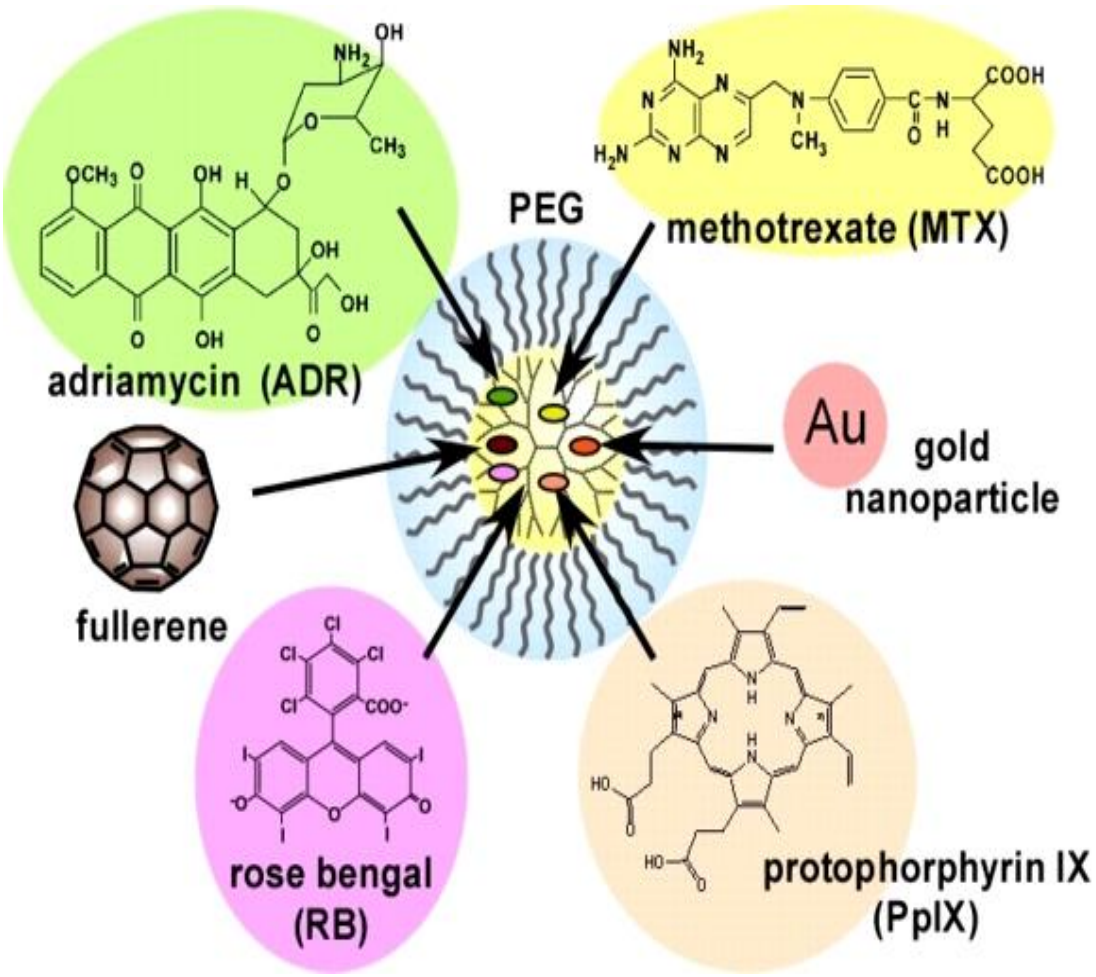

Figure 7 – Multiple materials introduced into PEGylated Dendrimer (*121*).

1.8.2 Advantages of PEGylation

PEGylation has many significant pharmacological advantages over the unmodified form by increasing the molecular weight of a molecule such as (*122*):

- Improved drug solubility
- Reduced dosage frequency, without diminished efficacy with potentially reduced toxicity
- Extended circulation lifetime
- Increased drug stability
- Enhanced protection from proteolytic degradation
- Water solubility
- High mobility in solution
- Lack of toxicity and low immunogenicity
- Altered distribution in the body

1.8.3 Limitations of PEGylation

PEG is attained by chemical synthesis and, like all synthetic polymers, it is polydispersed, with different number of monomers resulting in a Gaussian distribution of the molecular weights. This leads to a population of drug conjugates, with different biological properties, mainly in circulation time inside the body and immunogenicity.

A second problem reported with the use of this polymer is related with the renal clearance from the body. PEGs are usually excreted in urine or faeces but PEG with high molecular weights (>10000 k.Da) can long-term accumulate in the liver, leading to macromolecular syndrome (*110*).

1.9 Objectives and general strategies of the thesis

The main objective of the present project work was to synthesize degradable PEGylated dendrimer nanoclusters and investigate these nanosystems for delivery of an anticancer drug model, DOX. The nanoclusters were prepared via *in situ* crosslinking of low generation PAMAM dendrimers by *N,N'*-cystamine-bis-acrylamide (CBA) followed by PEGylation using carboxylated mPEG (molecular weight: 2000 g/mol). The synthesized compounds were characterized by using ^{1}H NMR and FTIR to confirm the polymerisation and PEGylation reaction (Figure 8). Size analysis and stability tests were performed for the synthesised particles for their effective use as drug delivery systems. Then, the drug release kinetics was studied *in vitro* using different pH conditions and reducible cell mimic conditions. Later, biological evaluation was performed by treating CAL-72 (osteosarcomal) cells with the drug-loaded nanosystems concerning their anticancer cytotoxicity and therapeutic efficacy. Cellular uptake tests were performed to check the internalization process of nanoclusters inside the cells and therapeutic accumulation intracellularly.

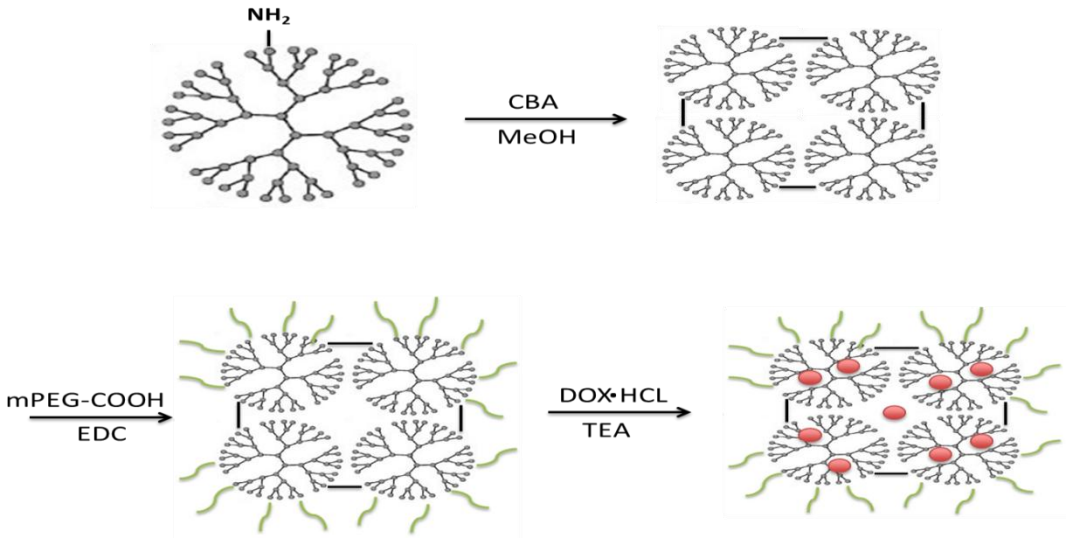

Figure – 8 Synthesis procedure of G3-CBA-PEG/DOX

CHAPTER 2 – MATERIALS AND METHODS

CHAPTER 2 – MATERIALS AND METHODS

2.1 Materials and Reagents

Generation 3 PAMAM dendrimers possessing ethylenediamine cores and amine termini (PAMAM G3 M.W. = 6909 g/mol with 32 NH_3 surface groups) in methanol solution, were purchased from Dendritech Inc. N, N'- Cystamine-bis-acrylamide (CBA, 98% purity) was purchased from SIGMA-ALDRICH. Triethylamine (TEA, purity > 99%) was purchased from MERCK. m-PEG-COOH was purchased from Yare Bio (China). Thioglycolic acid (TGA, purity 99%) was purchased from SIGMA-ALDRICH. Unless otherwise stated, all other chemicals were obtained from SIGMA-ALDRICH and used as received. Cell culture dishes were purchased from Nunc. The dialysis membranes were bought from Spectrum® labs and the filters used for solution sterilization were obtained from VWR™ with a pore size of 0.22 μm.

2.2 Synthesis of G3-CBA-PEG dendrimer nanoclusters

Crosslinking of PAMAM G3 dendrimer with N,N'-cystamine-bis-acrylamide (CBA) was carried out at 37 ^{o}C for 3 days.

The synthesis involves the following steps: PAMAM G3 (20 mg, 0.002894 mmol) was dissolved using 1 mL of methanol in an eppendorf. In another eppendorf CBA (0.75 mg, 0.002894 mmol) (1:1 mmol ratio) was dissolved in 1 mL of methanol. Then the dissolved CBA solution was dropwisely added to PAMAM G3 dendrimer solution at room temperature carefully using a micropipette. The reaction mixture was kept at 37^0 C for three days for the reaction completion. The finally formed reaction mixture was dialysed against Phosphate Buffered Saline (PBS) (pH 7.4, 3 times 3 L) through a dialysis membrane (Molecular Weight Cut Off (MWCO) of 2000 Da) for 24 hours, and against distilled water (3L 3 times a day) for two days to remove methanol and free CBA molecules. This was followed by lyophilization for 3 days to get G3-CBA dendrimer nanoclusters.

The final product (G3-CBA dendrimer nanoclusters) was analysed with ^{1}H NMR to confirm the successful reaction of CBA with G3 PAMAM.

2.3 The effect of CBA/G3 ratio on the formation of the dendrimer nanoclusters

Different ratios of CBA to PAMAM G3 were used (1:1, 1:2, 1:3 and 1:4) to study the effect of CBA and the content of disulphide linkage on the drug release properties, cytobiocompatibilty and the cytotoxicity. The synthesis was performed using the process mentioned above in Section 2.2. The materials required for the synthesis are shown in Table 1.

Table 1 – Materials required for the synthesis of G3-CBA dendrimer nanoclusters with different ratios of CBA (amount of methanol used in all assays: 2 mL).

Ratio (G3:CBA)	Amount of G3-PAMAM mmol	Amount of CBA mmol
1:1	0.002894	0.002894
1:2	0.002894	0.005788
1:3	0.002894	0.008682
1:4	0.002894	0.01157

2.4 PEGylation of G3-CBA

mPEG-COOH (molecular weight 2000 g/mol) was used to PEGylate the synthesised G3-CBA dendrimer nanoclusters. mPEG-COOH (0.036185 mmol) in the 1:5 molar ratio of G3:mPEG was dissolved in 1.5 mL of water. The terminal OH groups of the mPEG-COOH were activated using 1-ethyl-3-(3-dimethylaminopropyl) carbodiimide (EDC) (0.108554 mmol) dissolved in 1.5 mL of water. The EDC solution was then added in a dropwise manner using a micropipette. Then the reaction mixture was kept at room temperature for 3 h with continuous moderate stirring to activate the –COOH group of the mPEG-COOH. Then, the addition of G3-CBA (50 mg) in 1 mL of water was dropwisely added to the activated mPEG-COOH solution mixture. The reaction was carried out for 3 days at room temperature with continuous moderate stirring. The final compound obtained was then dialysed using a dialysis membrane (MWCO of 2000 Da) against distilled water (3 times 3L) for 3 days to remove the excessive by-products, followed by lyophilization for 3 days to obtain the G3-CBA-PEG dendrimer samples in a white solid state. The chemicals used for the PEGylation reaction are mentioned in Table 2.

Table 2 – Feed ratio for the PEGylation of G3-CBA dendrimer nanoclusters.

Chemicals	Mw, g/mol	Weight mg	mmol	Mol ratio	UP water, ml
G3*	6909	50.000	0.007237	1	1
mPEG-COOH (2000)	2000	72.369	0.036185	1:5	1.5
EDC	155.24	16.852	0.108554	1:15	1.5

G3* is the base quantity of the chemical used, the ratios of mPEG and EDC were taken as mentioned above in mmol ratio to G3 ratio.

2.5 Characterization of G3-CBA-PEG dendrimer nanoclusters

^{1}H NMR spectra of the final product G3-CBA-PEG and the intermediate product (G3-CBA) were recorded using a Bruker Advance II+ 400MHz NMR spectrometer. 0.4-0.5 mg of the samples was dissolved in 500-600 μL D_2O before measurements. FTIR analysis (Perkin Elmer Spectrum II) was performed for all the starting materials (G3-PAMAM, CBA and mPEG-COOH), the intermediate products (G3-CBA) and the final product G3-CBA-PEG. Samples were vigorously mixed by grinding the samples (G3-PAMAM, CBA, and G3-CBA-PEG) with KBr using ratio of 1:5 and were then subjected under hydraulic pressure of 10 tons to prepare pellets or disks for analysis using FTIR.

Analysis of encapsulation of DOX into the dendrimer nanoclusters was performed by UV-Vis spectra using a Lambda 2 UV-Vis spectrometer (Perkin-Elmer). Before measurement, samples containing DOX were dissolved in methanol.

2.6 Study of size and stability of synthesized compounds

Size measurements were performed for the samples (G3-CBA-PEG 1:1, 1:2, 1:3, 1:4 and G3-CBA-PEG/DOX 1:1, 1:2, 1:3, 1:4) to measure the hydrodynamic size of the modified dendrimers at pH 7.0, using a Zetasizer (Malvern). Samples were dissolved in 1 mL of PBS (pH 7.4) before the measurements.

100 μg of the samples were dissolved in 1 mL of water and were well-sealed with parafilm and were kept at room temperature. Hydrodynamic sizes of the particles (drug loaded and non-loaded) were measured after every 24 h for 10 days using the Zetasizer Nano ZS system.

2.7 Encapsulation of DOX within G3-CBA-PEG dendrimer nanoclusters

G3-CBA-PEG dendrimer nanoclusters (3 mg) were dissolved in 1 mL water. Doxorubicin hydrochloride (DOX · HCl) with 10 molar equivalents of dendrimers was dissolved in 150 μL methanol followed by adding 5 μL TEA to generate non-protonated DOX (*130*). Then the dendrimer aqueous solution was added carefully in a dropwise manner to the non-protonated

DOX solution and was stirred vigorously for 12 h, allowing the evaporation of the methanol solvent. After that, the solution mixture was centrifuged at 23 ^{o}C (10000 rpm for 10 min) in order to remove the precipitates, which were due to non-complexed free DOX. The supernatant was removed carefully and was lyophilized for 3 days to obtain the G3-CBA-PEG/DOX complex. The precipitate obtained was preserved and re-dissolved into 8 mL methanol for indirect determination of the encapsulated amount of DOX by UV-Vis analysis. The DOX loading process of G3 was similar except replacing G3-CBA-PEG with G3, and the obtained G3/DOX was used as control sample for further study.

The encapsulation efficiency of the dendrimer nanoclusters were calculated using the formula

1) $$\text{Unencapsulation} = \frac{\text{Average absorbance X Vol. of methanol}}{\text{Standard absorbance of DOX in methanol at 490 nm}} \Big/ \text{Amount of DOX used}$$

2) Encapsulation = Amount of the DOX used – Unencapsulation

3) Encapsulation Efficiency = 100 X Encapsulation / Amount of DOX used

The Loading Capacity of the synthesized dendrimer nanoclusters were calculated using the formula

4) Loading Capacity = Encapsulation (mg) / Weight of the sample obtained after lyophilization

2.8 In vitro drug release kinetic studies

Drug release tests were conducted for the samples of G3-CBA-PEG/DOX using G3/DOX as a control sample. The samples were filtered using a 0.22 μm filter, and then 10 μg of the sample was dissolved in 0.5 mL of water and was contained in a dialysis membrane (Spectrum® labs) of MWCO of 3500 Da. The dialysis bag was sealed and suspended into 5 mL of PBS at different pH (5, 6.5 and 7.4). All the systems were kept at 37 °C. At specific time points (1, 2, 4, 6, 8, 24, 48, 120, 216, 312, 456, 552, 840, 1008, 1128 hrs), 100 μL of the buffer medium was taken out for analysis and the volume replenished with the corresponding buffer solution

then, the aliquots were taken and read at 590 nm using a micro plate reader. A fluorescence spectrophotometer (model Victor3TM 1420, PerkinElmer) was used to determine the DOX content in the removed aliquots. The redox-sensitivity of the nanosystems was investigated in the presence of different concentrations of TGA (0.05, 0.1, 1 and 2 mM) to study their release behaviours.

2.9 Biological evaluation

Cal-72 cells (an osteosarcoma cell line) were continuously grown in the cell culture dishes with Dulbecco's Modified Eagle Medium (DMEM) supplemented with 10% fetal bovine serum (FBS), 1% (v/v) of antibiotic and antimycotic 100x solution (AA), 1% (v/v) of L-Glutamine (Glut) 100x. All the reagents mentioned here were purchased from Gibco. The culture was maintained at 37 °C under humid conditions in incubator with 5 % CO_2, and the medium was replaced every 3 days.

To check if the G3-CBA-PEG/DOX nanoclusters are therapeutically active, one day before experiments, cells were plated into 48-well plates at a density of 1×10^4 cells per well in the DMEM complete medium. The next day, the medium was replaced with fresh DMEM complete medium containing free DOX · HCl (5 μM) and G3-CBA-PEG/DOX complex at the same DOX concentration in PBS buffer (10 μL) and then the cells were incubated for 48 h at 37 °C. After treatment with DOX or dendrimer/DOX complexes, cell morphology was observed by optical microscopy (Nikon Eclipse TE 2000E inverted microscope). The magnification was set at 100× for all samples.

Resazurin assay (also known as Alamar Blue assay) was performed to the cells to quantify the viability. Resazurin solution was added in an amount equal to 10% of the culture medium volume and the cultures were kept in incubator for 2-4 h. Samples can be measured spectrophotometrically by monitoring the decrease in absorbance at a wavelength of 600 nm. Alternatively, samples can also be measured fluorochrome spectrophotometrically by monitoring the increase in fluorescence at a wavelength of 590 nm using an excitation wavelength of 560 nm. Each test included a blank containing complete medium without cells. After that, the cells were washed 2 times with PBS (pH 7.4) and 3 times with distilled water and were analysed using (Nikon Eclipse TE 2000E inverted microscope).

For the cell uptake study, cells were plated for 24 h before the incubation. Freshly prepared PBS, solutions of DOX, G3/DOX, and samples of G3-CBA-PEG/DOX with different G3:CBA ratios (1:1, 1:2, 1:3, 1:4) with an equivalent DOX concentration (0.5 μM) were then added to the cells and were kept at 37 ºC for 2 and 4 h, respectively. Subsequently, the cells have to be washed with sterilized PBS buffer and, simultaneously, fixed with 3.7% (v/v) formaldehyde solution and stained with 4',6-diamidino-2-phenylindole (DAPI, Sigma) for 30 min to stain the nucleus of the cells. The cells then were washed with PBS solution for further analysis by optical fluorescence microscopy (Nikon Eclipse TE 2000E inverted microscope).

Note: For the encapsulation of DOX and drug release studies, water-insoluble DOX was used, while for cell biological evaluation, water-soluble DOX.HCl was used as a control to check the therapeutic activity of the free drug.

CHAPTER 3 – RESULTS AND DISCUSSION

3.1 Synthesis and characterization of G3-CBA-PEG dendrimer nanoclusters

G3 PAMAM dendrimers are smaller in size with fewer impurities when compared with higher generation dendrimers. These dendrimers show low cytotoxicity when compared with the higher generation dendrimers (*85*). The terminal groups of CBA react with the NH_2 terminal groups of dendrimers resulting in the formation of dendrimer nanoclusters. The disulphide crosslink acts as a bridge between two dendrimer units. The most important advantage of using this disulphide crosslinked molecule is the degradability when reacted with the glutamic groups present inside the cell providing easy release of the drug encapsulated in the nanoclusters (*104*). The polymerization reaction is shown in Figure 9.

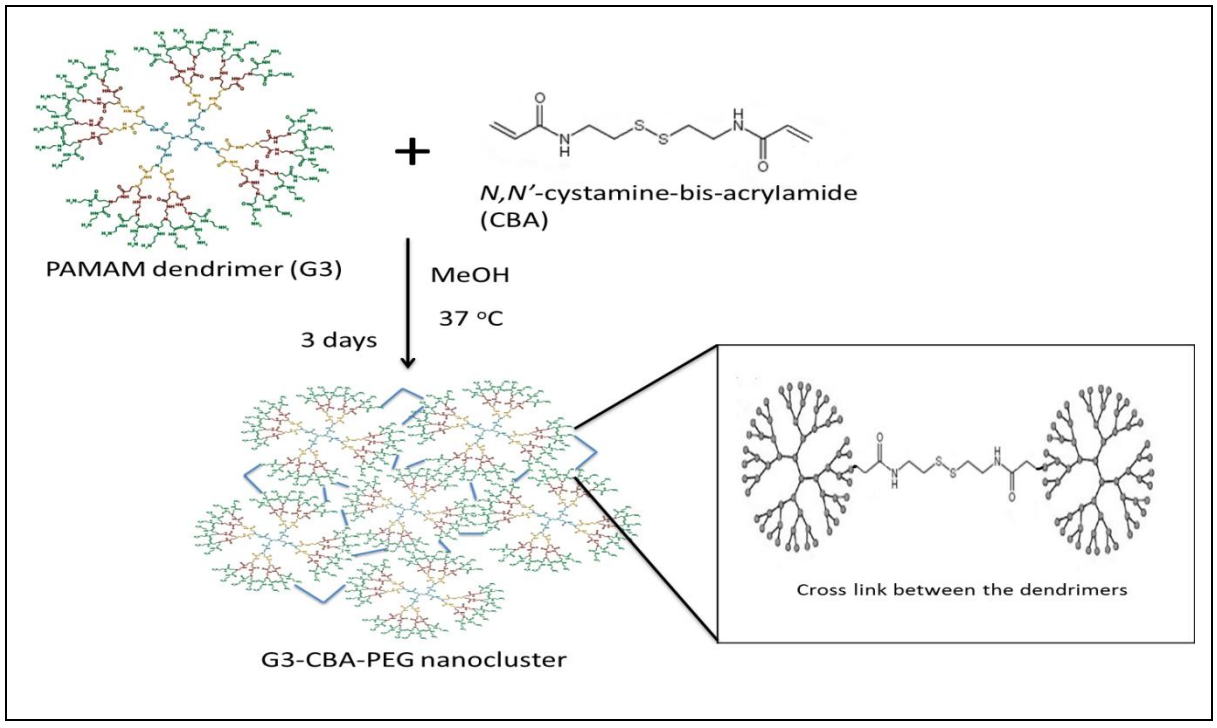

Figure 9 – Schematic representation of development of G3-CBA nanoclusters via *in situ* crosslinking of G3 with *N,N'*-cystamine-bis-acrylamide (CBA).

The second major step involved in the synthesis was to PEGylate the formed dendrimer nanoclusters. But, before the PEGylation reaction, the terminal groups of mPEG were activated using EDC for 3 h and the solution mixture was directly added to the solution containing G3-CBA dissolved in Ultra-pure water. The reaction mechanisms involved in the

activation of the carboxylic groups of mPEG-COOH are shown in Figure 10. The by-products (isourea) and excess reagents from the reaction mixture were removed by dialysis (*122*).

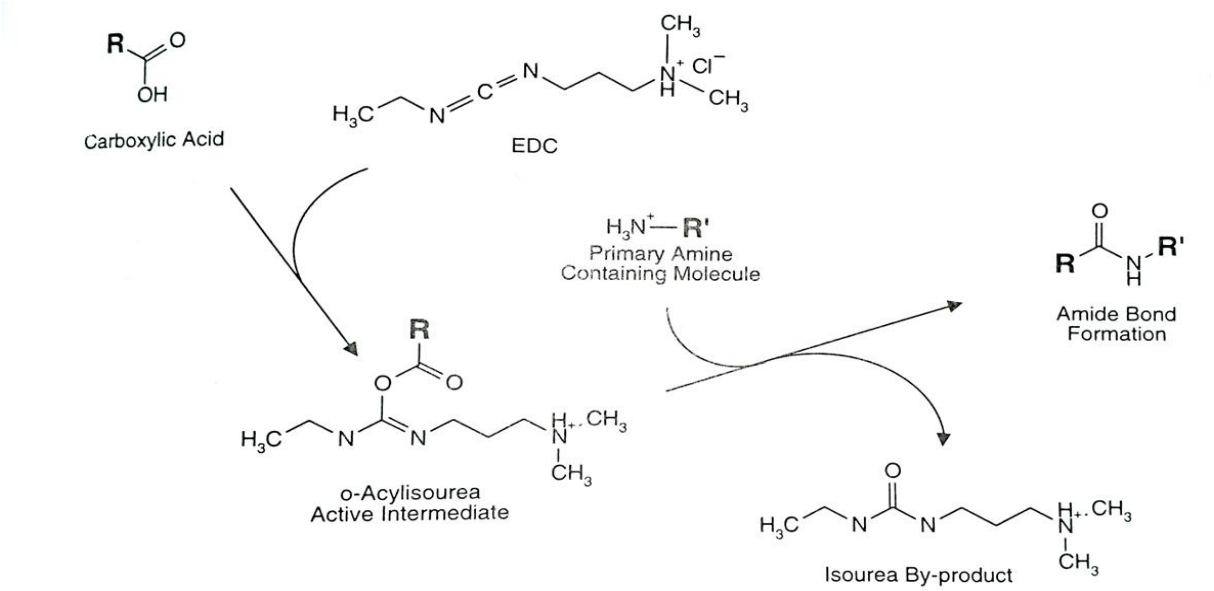

Figure 10 – Schematic representation of the reaction steps involved in the activation of carboxylic acid groups of mPEG-COOH by EDC (*123*).

After the activation of the terminal groups of mPEG, the solution was mixed with the G3/CBA dendrimer nanoclusters to synthesize the final compound G3-CBA-PEG dendrimer nanocluster. CBA is attached covalently to the dendrimer and moreover mPEG-COOH chains may provide the cover for the drug encapsulated and increase the circulation time of the nanoclusters inside the body (*124*). Another advantage of using mPEG-COOH is to improve the solubility and colloidal stability of the nanoclusters in the medium (*125*). The PEGylation reaction involved in the synthesis of G3-CBA-PEG nanoclusters is shown in Figure 11.

After the reaction was completed, the final compound obtained after dialysis and lyophilization was a white solid of G3-CBA-PEG dendrimer nanoclusters.

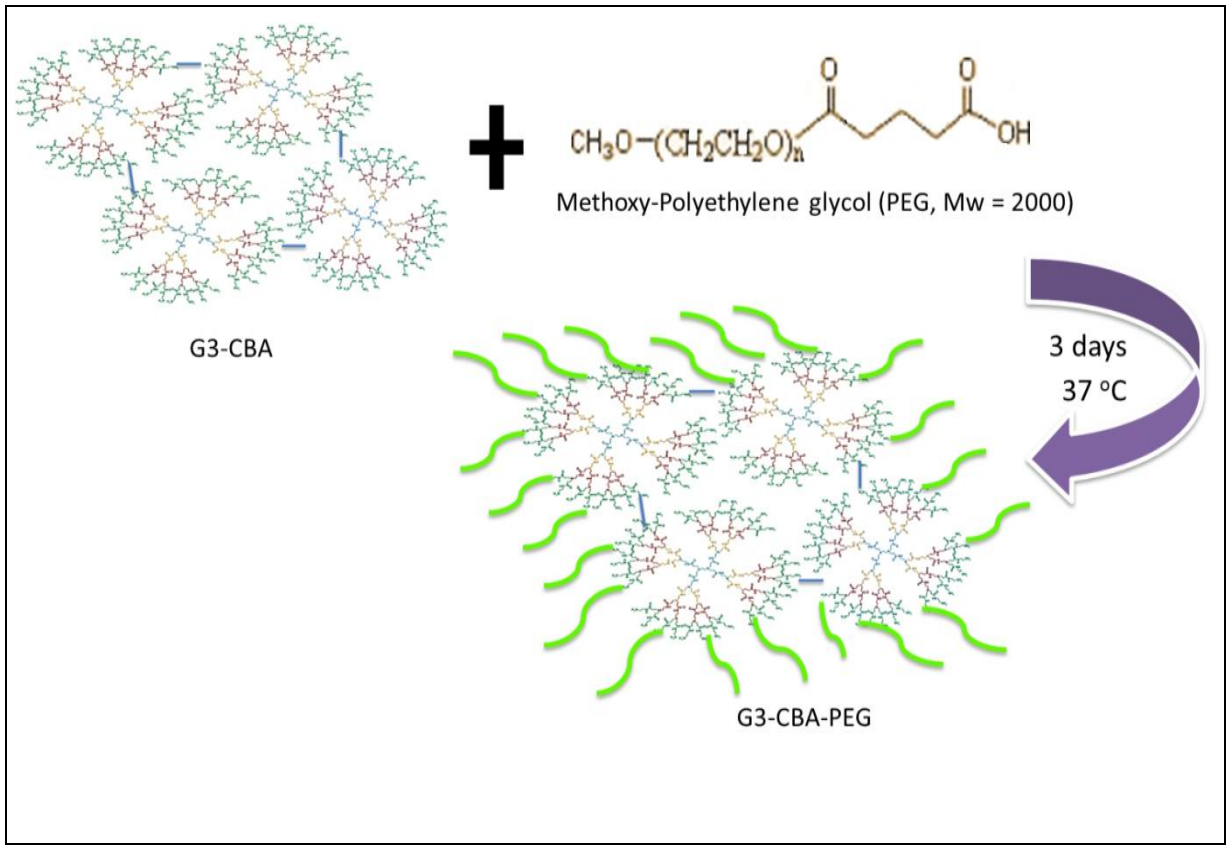

Figure 11 – PEGylation of G3-CBA dendrimer nanoclusters.

3.1.1 Characterisation by ^{1}H NMR

The first reaction step was to synthesize G3-CBA dendrimer nanoclusters (Figure 9). The nanoclusters were then characterised by ^{1}H NMR and FTIR. In the ^{1}H NMR spectrum of G3-CBA in D_2O (Figure 12), we can see the peaks of CBA protons, (δ=3.41 ppm NHC*H*$_2$CH$_2$S-S, 4H) (*126*). The high intensity of the peak can be observed due to the overlapping of the peaks from protons of G3-PAMAM (δ=3.46 CONHC*H*$_2$) with the protons of CBA as both the protons have the same adjacent NH group. After purification with the dialysis of the final compound, we suppose that the entire methanol from the compound was removed as no specific peak of methyl protons were observed in the spectrum. We also suppose that the characteristic peaks representing the CBA are the linked peaks to the dendrimers and all the unreacted CBA molecules were removed. Thus, based on the integration, we calculated that 0.92 molecules of CBA were linked with each dendrimer using G3-PAMAM dendrimer peaks as reference.

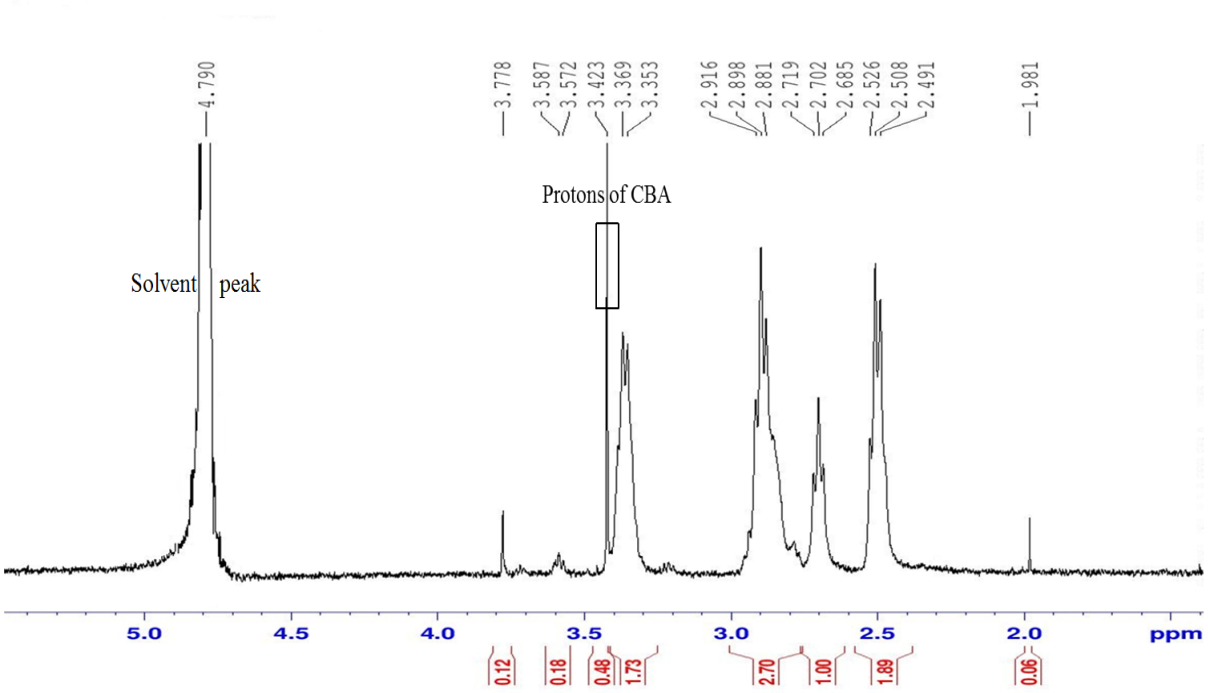

Figure 12 – ^{1}H NMR spectrum of G3-CBA Dendrimer nanoclusters.

In the second step of the reaction (PEGylation), G3-CBA-PEG dendrimer nanoclusters were synthesized (Figure 10). In the ^{1}H NMR spectrum of G3-CBA-PEG in D_2O (Figure 13), we can see the characteristic peak of the mPEG protons (–O–CH_2CH_2 δ=3.71 ppm) (*127*). We assume that the mPEG molecules were interacted covalently and the free unreacted PEG were removed during the dialysis. Considering the ^{1}H NMR spectra (Figure 12 and 13) we can confirm that the reaction was successful and the final product G3-CBA-PEG dendrimer nanoclusters were obtained.

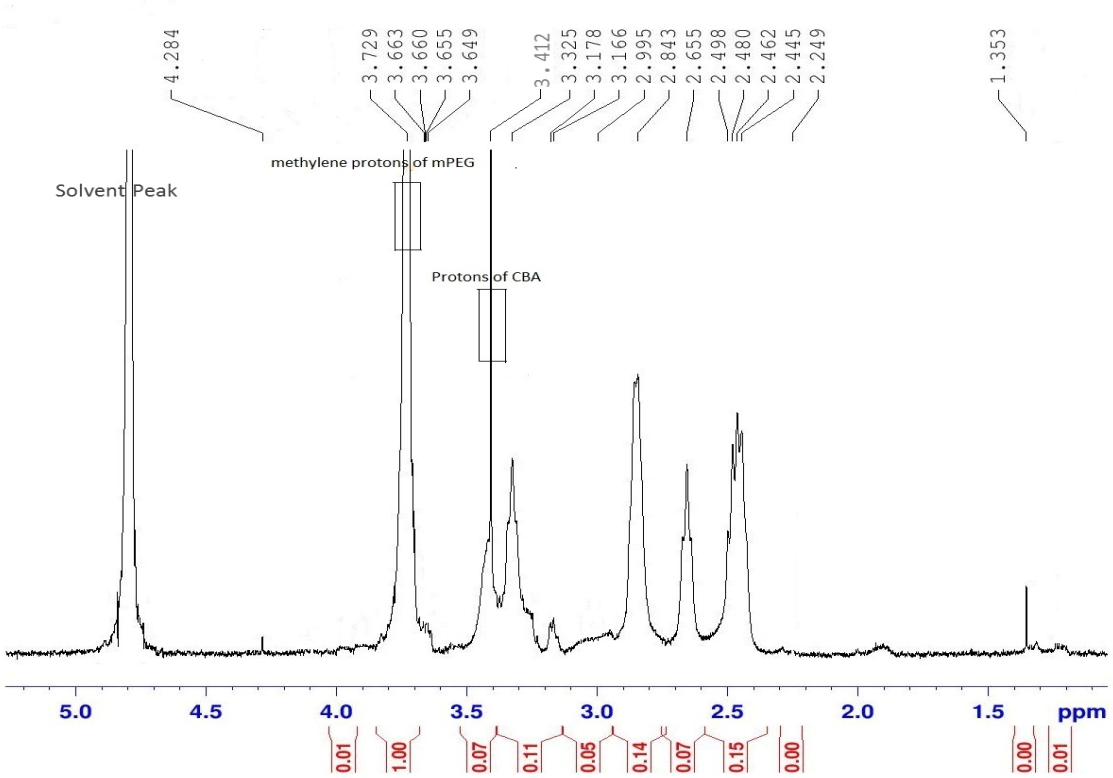

Figure 13 – ^{1}H NMR spectrum of G3-CBA-PEG Dendrimer nanoclusters.

G3-CBA-PEG dendrimer nanoclusters were then synthesised using different ratios of dendrimer to CBA (1:1, 1:2, 1:3 and 1:4). The ^{1}H NMR spectrum of all the samples (G3-CBA-PEG 1:1, G3-CBA-PEG 1:2, G3-CBA-PEG 1:3, G3-CBA-PEG 1:4) shows that the reaction was successful as we can see the characteristic peaks of CBA ($NHCH_2CH_2S$-S, group δ=3.41 ppm) (*126*) and the characteristic peaks of mPEG (–O–CH_2CH_2 δ=3.71 ppm) (*127*) in the spectrum (Figure 14). The ^{1}H NMR spectra of the samples show no shift between the compounds. The peaks obtained at δ= 1.353 ppm and δ= 4. 284 ppm may be the peaks from any intermediate by-products or from the impurities during the PEGylation reaction which can be observed in the spectrum. The ratios of CBA to dendrimer obtained were very less than expected when calculated based on ^{1}H NMR spectrum. The obtained ratio of CBA to dendrimer is shown in Table 3.

The most important reason for this result is due to the formation of clusters with some active reactive sites left inside the cluster, further not reacting with the CBA molecules. The conversion rate is normal, since not all CBA will react with the amino groups due to the limitation of the reactivity under the current synthetic conditions.

Table 3 – Calculated ratios of G3-CBA dendrimer nanoclusters.

CBA ratios calculated for the reaction	Expected Ratios	Calculated ratios of CBA
1:1	1	0.92
1:2	2	1.21
1:3	3	1.48
1:4	4	1.79

The ratios of mPEG to the dendrimer were also found to be very less when compared with the ratio used for the synthesis. The possible explanation for this phenomenon may be due to the insufficient reactive groups left on the pheriphery of the dendrimer after polymerisation with CBA. Another reason resulting in the lower ratio can be caused during the activation of terminal carboxylic groups of mPEG where not all the terminal groups were activated. The obtained mPEG ratios to dendrimer are mentioned below in Table 4.

Table 4 – Calculated ratios of G3-CBA-PEG dendrimer nanoclusters.

G3-CBA ratios	mPEG ratios calculated for reaction G3: mPEG	Obtained G3:mPEG ratio
1:1	1:5	1:2.4
1:2	1:5	1:2.4
1:3	1:5	1:2.3
1:4	1:5	1:2.2

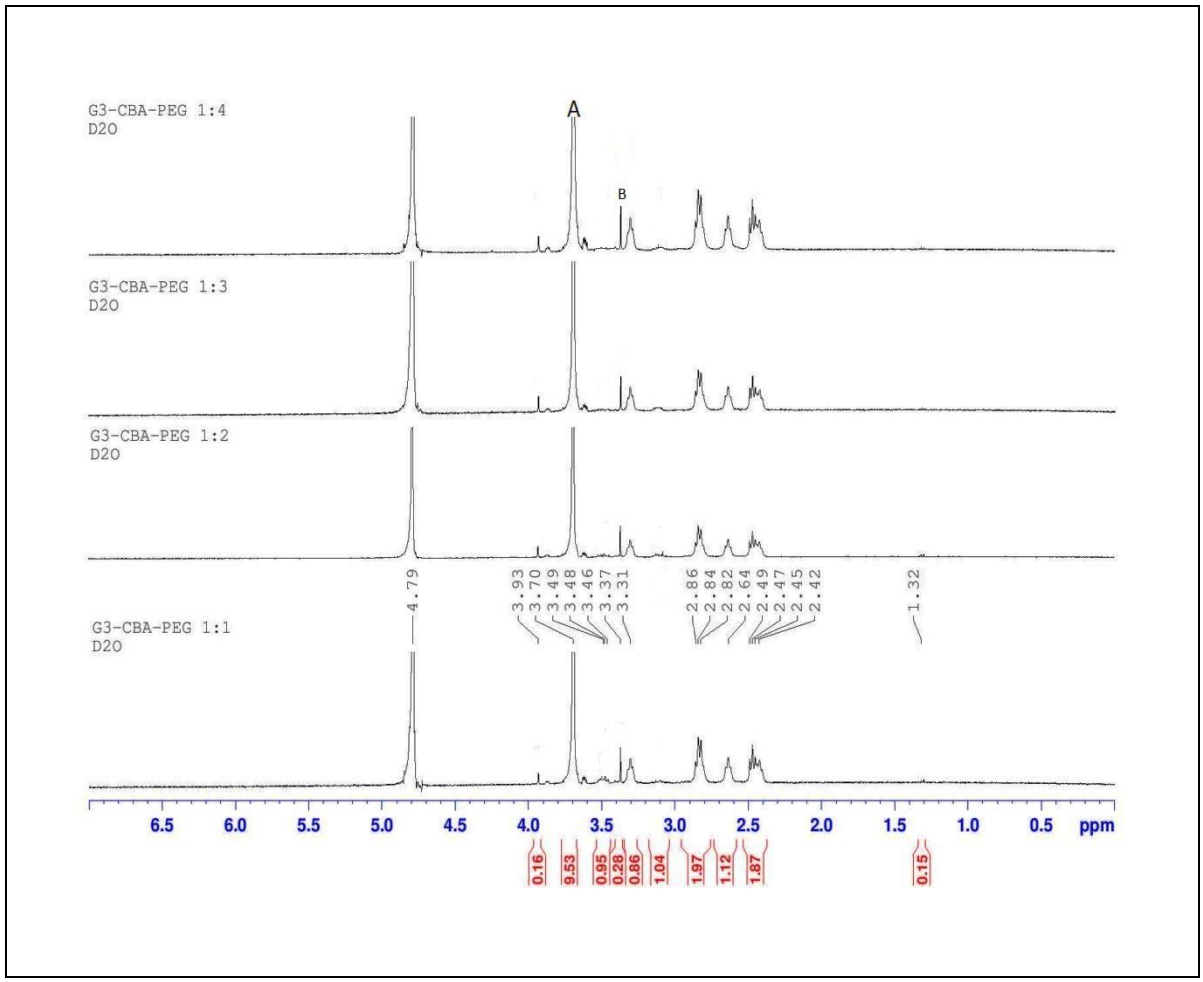

Figure 14 – ^{1}H NMR spectrum of G3-CBA-PEG dendrimer nanoclusters at different ratios, from the bottom to top (1:1, 1:2, 1:3, and 1:4). Peak A is the characteristic peak of PEG as shown in Figure 13 and peak B is the characteristic peak of CBA as shown in Figure 12.

3.1.2 Characterisation by FTIR

To confirm the conjugation of CBA/dendrimers and their following PEGylation reactions, FTIR analysis was also performed for the final product G3-CBA-PEG dendrimer nanoclusters and also for the intermediate compound (G3-CBA). In the FTIR spectrum (Figure 15) we can observe the characteristic peaks of the materials (G3-PAMAM, CBA and mPEG-COOH) which are used in the reaction. The detailed peak list is given below;

Characterstic peaks of mPEG (*128*):

O-H Stretching: 3441 cm^{-1}

C-H stretching: 2878 cm^{-1}

C-H extended stretching: 1464 and 1343 cm^{-1}

O-H and C-O-H stretching: 1279 and 1074 cm^{-1}

Characteristic peaks of G3-PAMAM dendrimer (*129*):

N-H band at 3280 cm^{-1}

C=O band at 1645 cm^{-1} and

N-H bending at 1556 cm^{-1}

Characteristic peaks of CBA S-S band at 1229 cm^{-1}

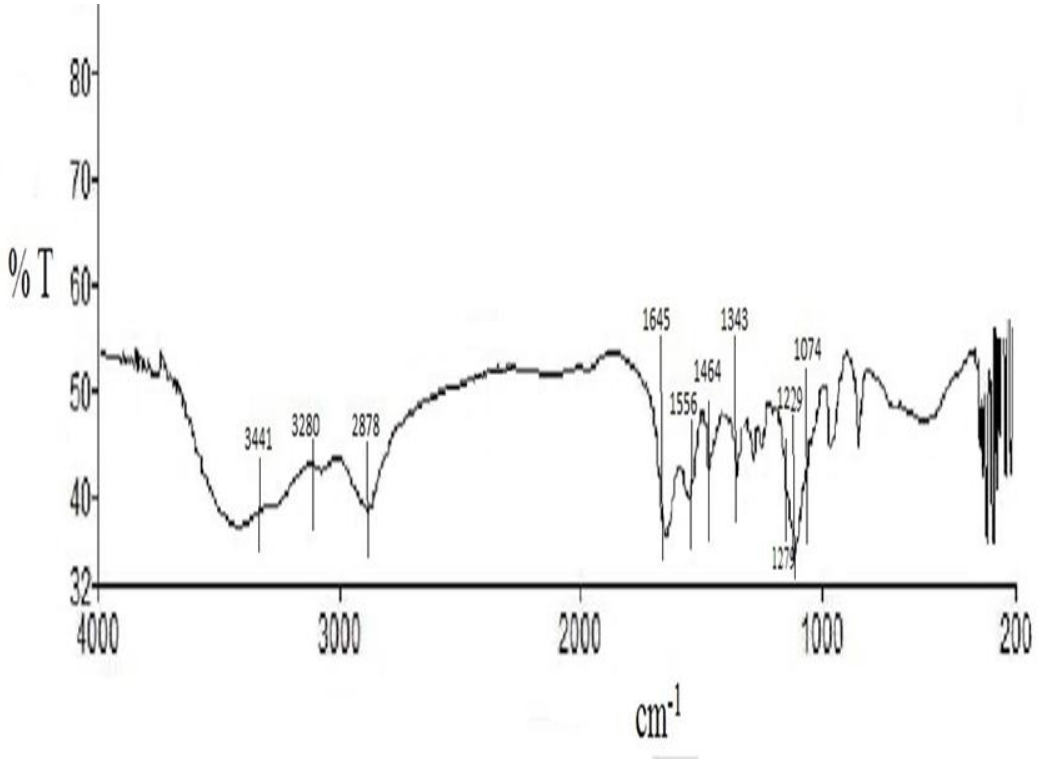

Figure 15 – FTIR spectrum of G3-CBA-PEG dendrimer nanoclusters.

The peak representing CBA show very less intensity in the compound G3-CBA-PEG when compared with the free CBA peak due to the formation of clusters. The detailed spectrum and peak integration of the starting materials (G3-PAMAM, CBA and mPEG-COOH) and the intermediate compounds are shown in ANNEX II (Figure 30, 31 and 32).

3.2 Analysis of encapsulation of DOX to G3-CBA-PEG dendrimer nanoclusters

Encapsulation of DOX in the G3-CBA-PEG dendrimer nanoclusters was performed using the procedure reported by Xiangyang Shi et Al. (*130*) (Figure 16). The encapsulation efficiency and the loading capacity were studied using UV-Visible spectroscopy considering G3-PAMAM/DOX as the control sample. The encapsulation efficiency of G3-CBA-PEG increased when compared to that of G3/DOX (Figure 17) but when the ratio of CBA to dendrimer increased, the encapsulation efficiency of DOX gradually decreased. We suspect this phenomenon is due to the formation of nanoclusters of large size. When the sizes of the nanoclusters are increased, the surface area decreases which results in the poor adsorption of the drug on the surface of the nanoclusters. Another reason can be the close packing of the nanoclusters which prevents the entry of drug resulting in poor encapsulation. The encapsulation efficiencies of G3-CBA-PEG/DOX at different ratios are shown (Table 5). The loading capacity of G3/DOX and G3-CBA-PEG/DOX were calculated based on the results of encapsulation efficiency and the total weight of the sample obtained after lyophilization. The results show that the loading capacity of G3-CBA-PEG/DOX increased when compared with G3/DOX, but gradually decreased when the ratio of CBA to dendrimer is increased (Figure 18).

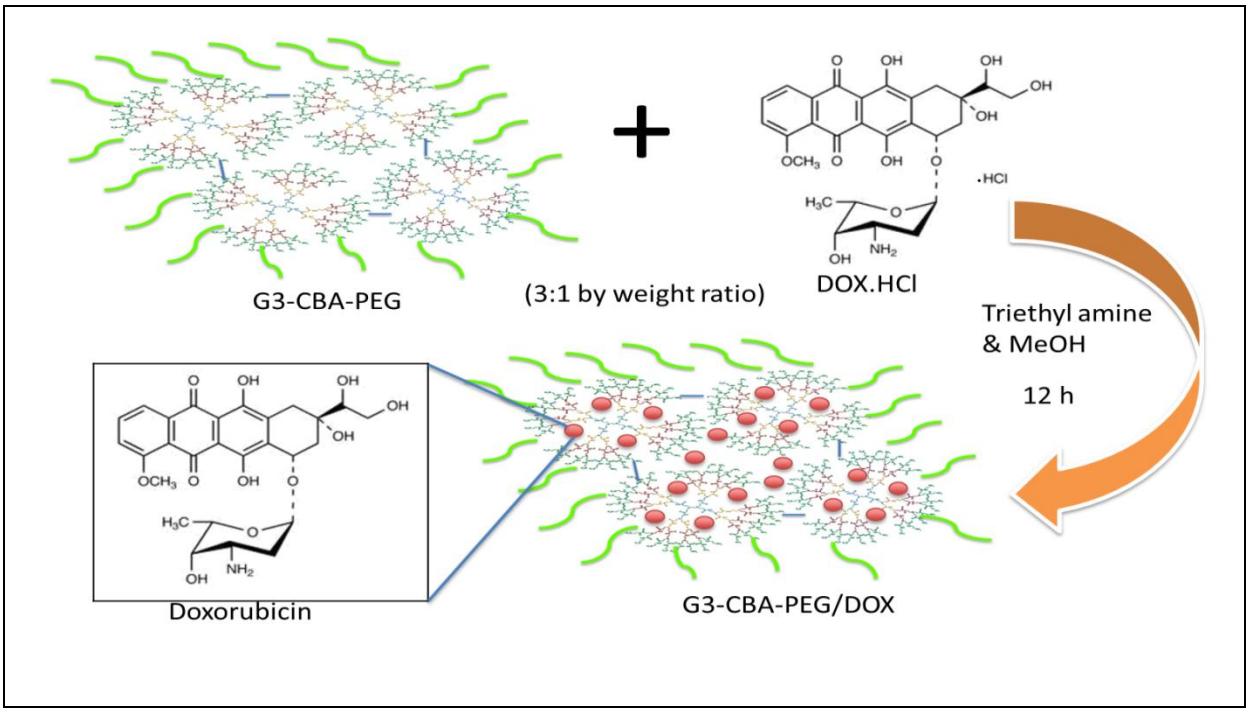

Figure – 16 Schematic representation of encapsulation of DOX to G3-CBA-PEG dendrimer nanoclusters.

Table 5 – Calculated encapsulation efficiencies of DOX for the compounds G3/DOX and G3-CBA-PEG/DOX at different ratios.

Name of the sample	Encapsulation efficiency, wt%
G3/DOX	63.56 ± 1.2
G3-CBA-PEG (1:1)	66.17 ± 0.4
G3-CBA-PEG (1:2)	57.36 ± 0.41
G3-CBA-PEG (1:3)	55.47 ± 0.25
G3-CBA-PEG (1:4)	53.34 ± 0.63

Note that the encapsulation of DOX to dendrimer nanoclusters was repeated for 3 times and the average values with standard deviations are reported.

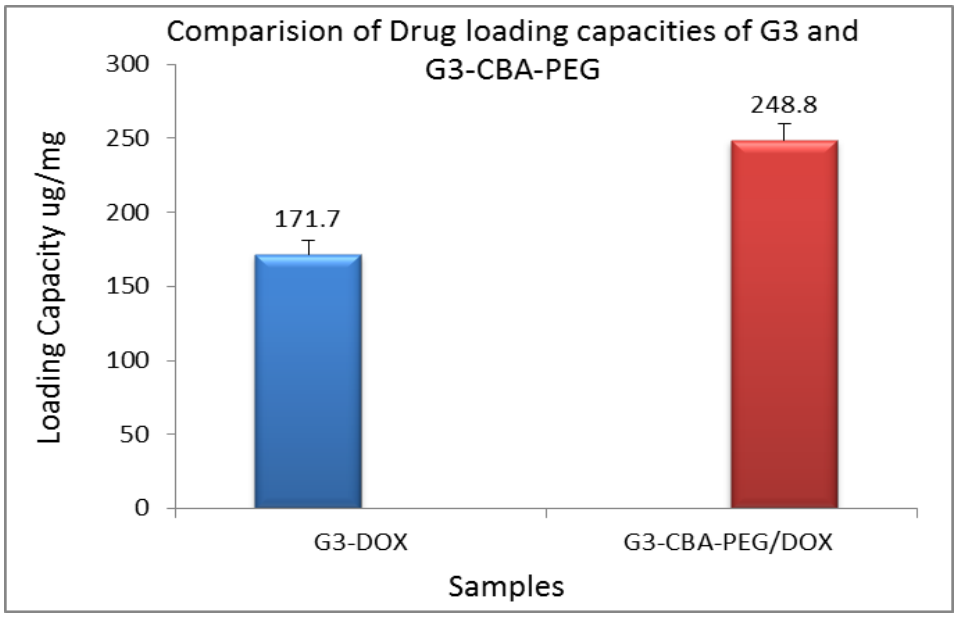

Figure 17 – Comparison of loading capacities of G3/DOX and G3-CBA-PEG/DOX.

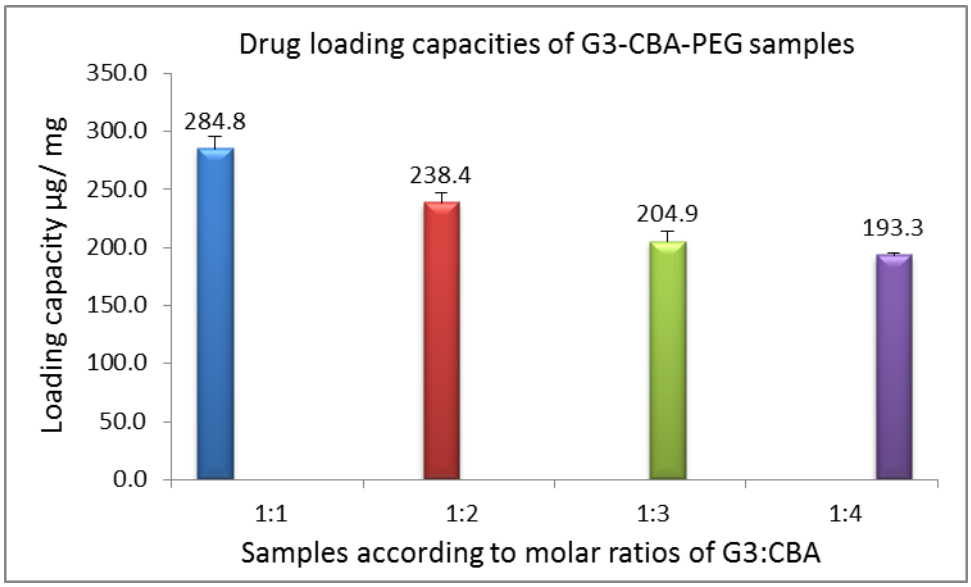

Figure 18 – Comparison of loading capacities of G3-CBA-PEG/DOX at different ratios.

3.3 Hydrodynamic analysis

The size analysis of G3-CBA-PEG and the drug encapsulated G3-CBA-PEG/DOX were measured using the dynamic light scattering (DLS) technique. The samples were filtered using a 0.22 µm filter before analysis. The temperature (23 ^{o}C) remained constant all along the analysis. The sizes of the samples increased with the ratio of CBA due to the formation of the clusters of higher radius for both drug free and drug loaded nanoclusters, which are shown in Figure 19 and Figure 20. When the ratio of CBA increased, more number of molecules react with the terminal groups of G3-PAMAM which bring other dendrimer units closer by crosslinking while forming the clusters. This results in the formation of clusters with bigger size. The increase in the size of the drug loaded nanoclusters is due to the formation of supramolecular assembly of the drug and dendrimer nanoclusters. The drug molecules perhaps have occupied the outer terminal space between the branches of dendrimers and the other molecules around the surface of the mPEG molecules which results in the increase of size when compared with drug non-loaded samples.

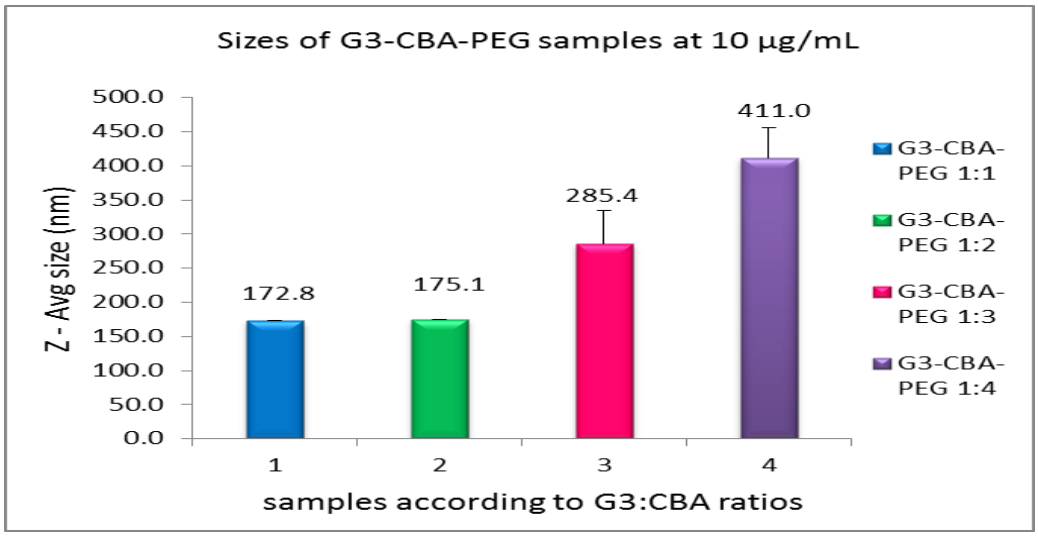

Figure 19 –Hydrodynamic sizes of G3-CBA-PEG samples at different ratios of CBA to dendrimer.

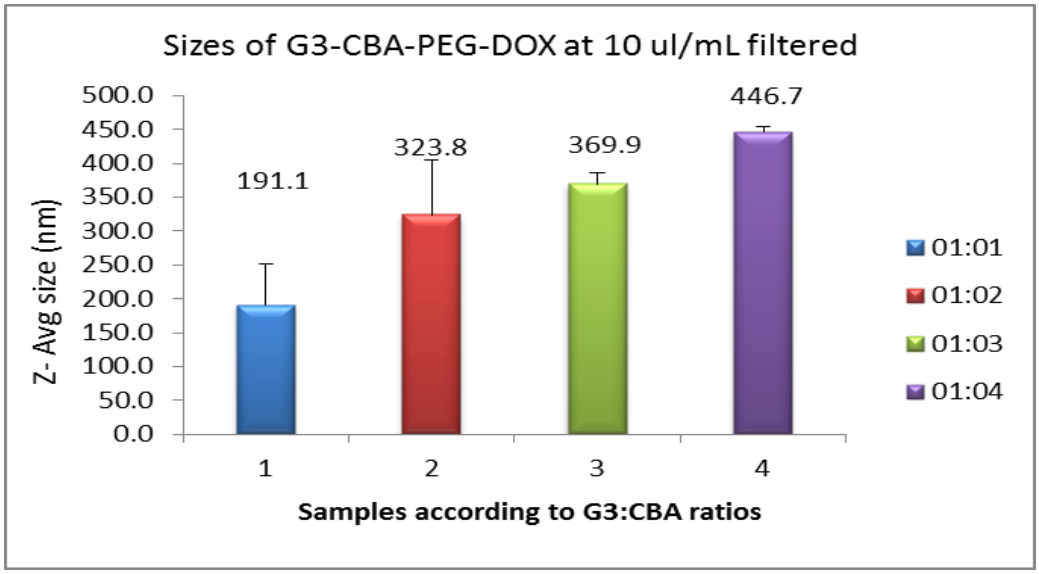

Figure 20 –Hydrodynamic sizes of G3-CBA-PEG/DOX samples at different ratios of CBA to dendrimer.

3.3.1 Study of stability of the synthesised NPs

100 µg of the G3-CBA-PEG (Figure 21) and G3-CBA-PEG/DOX (Figure 22) samples of different ratios were dissolved in 1 mL water and 1 mL PBS (pH 7.4) separately, and were kept at room temperature. The samples were analysed every 24 h for 7 days. The sizes of the

samples were measured at regular interval of time using DLS technique. No agglomerations of the particles were seen during this period and the sizes of the samples remained constant. From these data (ANNEX III), we can say that the samples are stable under similar physiological conditions observed in the body and will not agglomerate during the period of time and are capable of reaching the tumour cells without degrading. These types of systems can be promising vehicles for drug delivery.

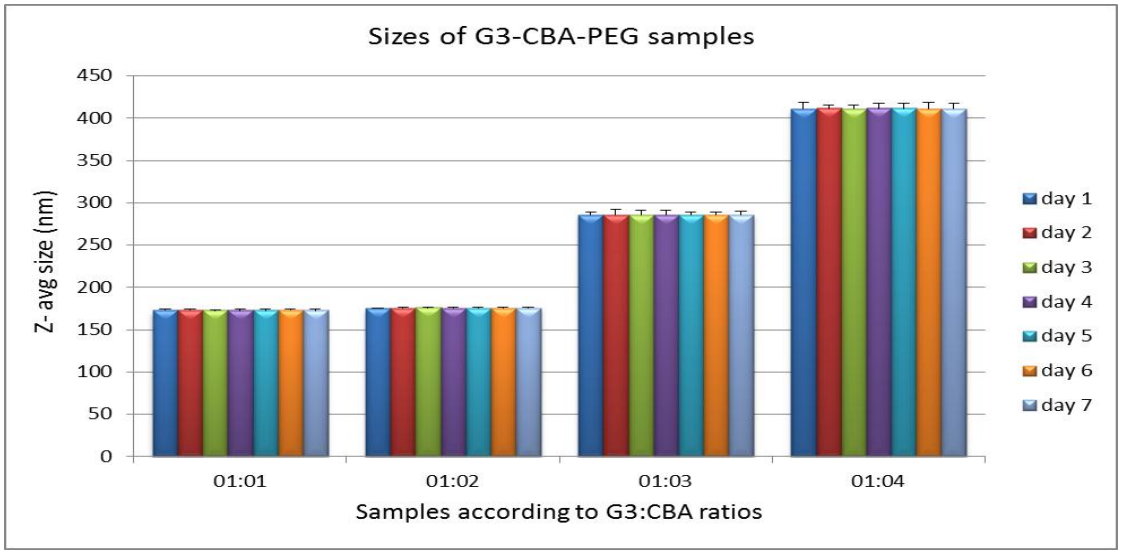

Figure 21 – Z-average sizes of G3-CBA-PEG (1:1, 1:2, 1:3, and 1:4) samples during a period of 7 days.

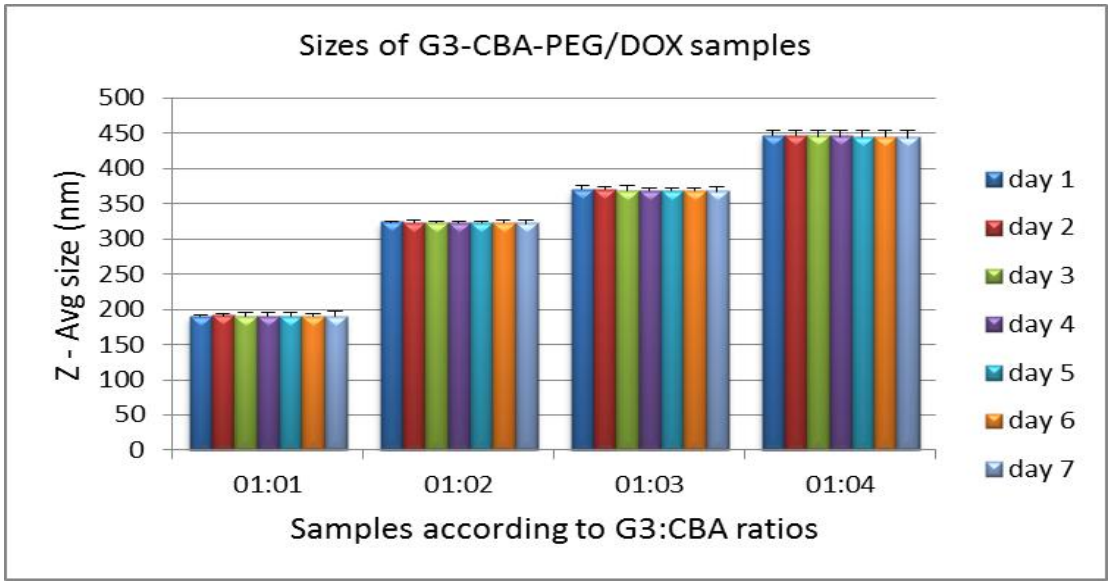

Figure 22 – Z-average sizes of G3-CBA-PEG/DOX (1:1, 1:2, 1:3, and 1:4) samples during a period of 7 days.

3.4 Evaluation of drug release in-vitro at different pH conditions

Drug release tests were performed for G3/DOX and G3-CBA-PEG/DOX samples to study their drug release behaviour's in PBS (pH 7.4, 6.5 and 5.0). The drug release profiles of G3/DOX and G3-CBA-PEG/DOX are shown in Figure 23 and Figure 24.

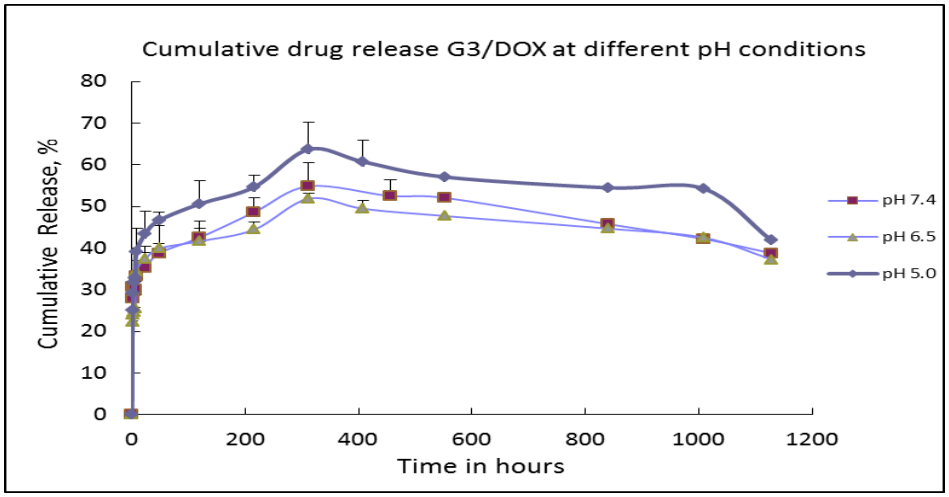

Figure 23 – Cumulative Drug release of DOX from G3/DOX in PBS buffer with different pH conditions at 37 ^{0}C.

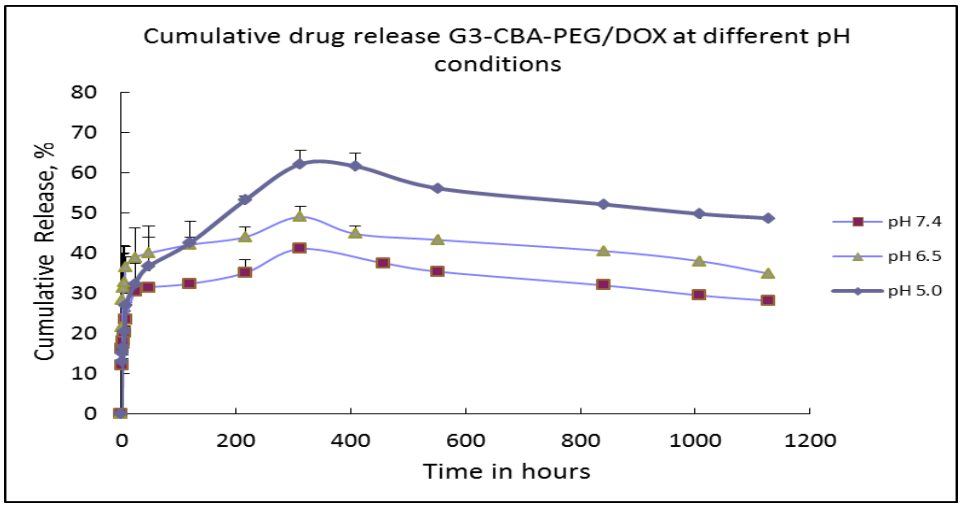

Figure 24 – Cumulative Drug release of DOX from G3-CBA-PEG/DOX (G3:CBA 1:1) at different pH conditions at 37 ^{0}C.

For the *in vitro* drug release studies the samples were sealed tightly using dialysis membrane (MWCO 3500) and were suspended into PBS buffers (pH 7.4, 6.5, and 5.0) and were

contained in 15 mL poly centrifuge tubes. The tubes containing the samples were kept in incubator at 37 ^{o}C.

For antitumor therapeutic applications, the encapsulated DOX should be effectively released into the cytoplasm and reach the nucleus to exert its biological activity (*131*). To understand the release ability of G3-CBA-PEG/DOX nanocomplexes, their cumulative release profiles were investigated in PBS solution at different pH values (7.4, 6.5, and 5.0), as a function of soaking time (Figure 24). On the other hand, the release of DOX from the G3-CBA-PEG/DOX seemed to be enhanced by decreasing the pH value, revealing that the nanocomplexes are pH sensitive. In this case, the G3-CBA-PEG/DOX offered a significantly accelerated DOX release ability at pH 6.5 (conditions mimicking the extracellular environment of a solid tumor) and pH 5.0 acidic conditions that mimic the endo-lysosomal internal milieu compared to that at physiological pH conditions, thus possibly to result in an improved drug release ability and anticancer efficacy.

3.4.1 Drug release kinetics at reducible intracellular mimic conditions

To understand the release rates of the synthesized compound in the body, drug release of G3-CBA-PEG/DOX was studied under reducible intracellular mimic conditions using TGA medium and G3/DOX (Figure 25) was kept as a standard to compare the release profiles. TGA medium have free thiol groups which provides the similar conditions observed in the cells. In 0.05mM TGA medium the sample G3-CBA-PEG/DOX showed enhanced release profile when compared with the release profile at normal PBS 7.4 (Figure 26). This is due to the reaction of the cross linkage present between the dendrimers. The disulphide cross link reacts instantly with the thiol groups present in the TGA medium, hence leading to the cleavage of the nanoclusters to promote the drug release (*94*). The release profile in TGA medium followed a biphasic pattern showing a rapid release in the beginning and a sustained release after a period of time.

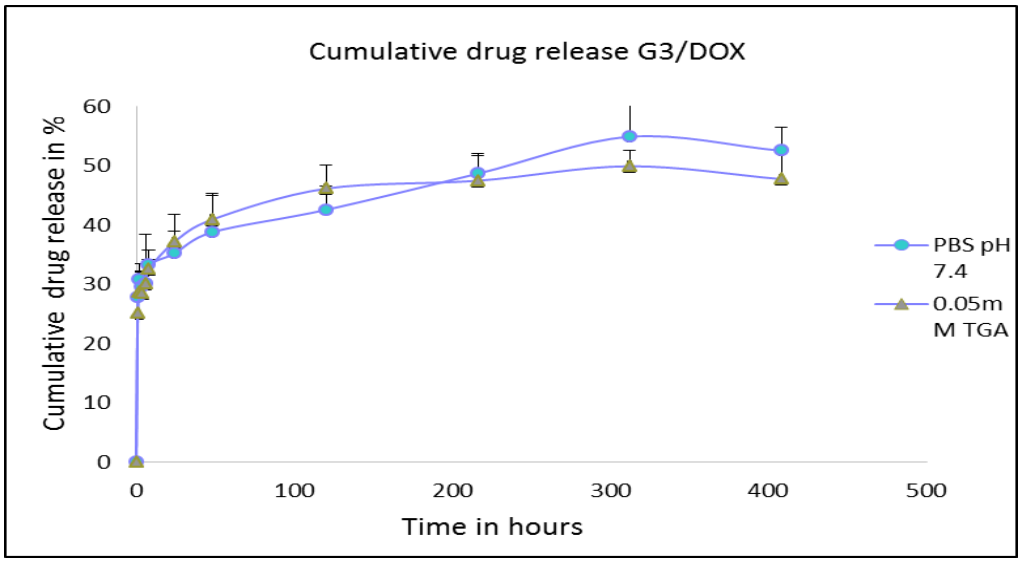

Figure 25 – Comparison of Cumulative drug release of DOX from G3/DOX in PBS buffer (pH 7.4) and 0.05 mM TGA medium.

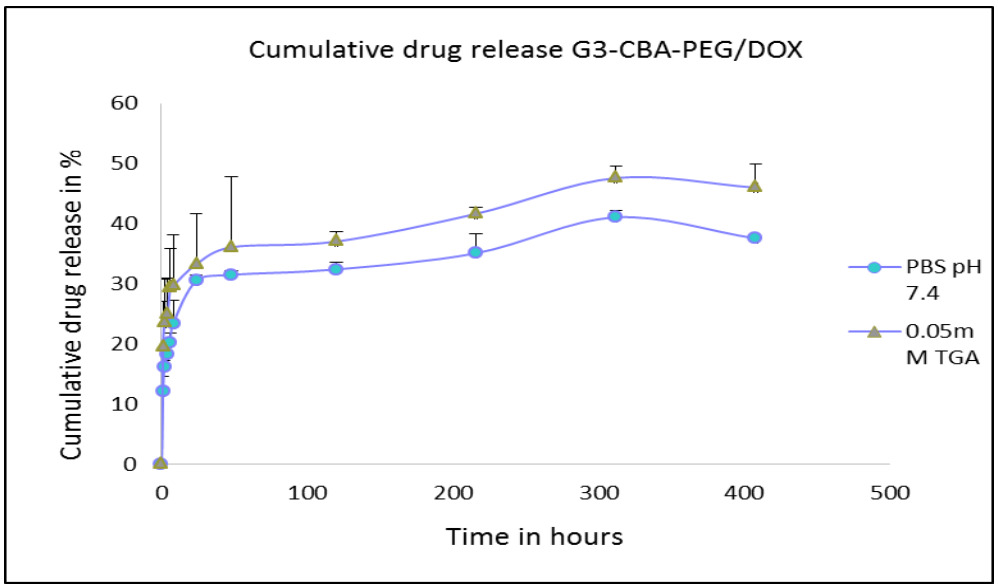

Figure 26 – Comparison of Cumulative drug release of DOX from G3-CBA-PEG/DOX (G3:CBA 1:1) in PBS buffer (pH 7.4) and 0.05 mM TGA medium.

The drug release was also conducted at different concentrations of TGA. As shown in Figure 35, the further increase of TGA concentration seems to result in a decrease of the whole absorbance intensity, possibly because higher TGA concentration produced a too much reducible environment to induce a modification of the DOX chemical structure. The complete drug release profile of G3/DOX and G3-CBA-PEG/DOX are presented in ANNEX

IV (Figure 34-42). The aliquots for the drug release studies were studied using fluorescence spectroscopy.

3.5 Evaluation of cytotoxicity

The cytotoxicity of the DOX-loaded nanocomplexes was quantitatively evaluated using CAL-72 cells (an osteosarcoma cell line) through the resazurin reduction assay (Figure 27). It can be seen that the cells treated with G3-CBA-PEG showed a higher viability than the corresponding G3 dendrimers, suggesting the introduction of the PEG onto the nanoclusters is helpful to improve the biocompatibility of G3. The G3-CBA-PEG/DOX nanoclusters exhibited an obviously higher anticancer cytotoxicity to CAL-72 cells than the corresponding drug free systems, suggesting that the cytotoxic effect was only due to the drug loaded within the nanocomplexes. The increase of CBA/G3 ratio seems to reduce the anticancer cytotoxicity of the DOX-loaded nanoclusters, probably because the high concentration of CBA which acts as crosslinker leads to the formation of a more compact structure, which limited the DOX release ability from the nanoclusters. Even though the cytotoxicity of G3/DOX was higher towards these cells as compared to G3-CBA-PEG/DOX, but, for *in vivo* applications, one should expect the latter could exhibit a longer circulation period than the former due to the presence of PEG, thus possibly resulting in a higher effect on the tumor site due to the prolonged EPR effect (*92, 94, 120, 122*).

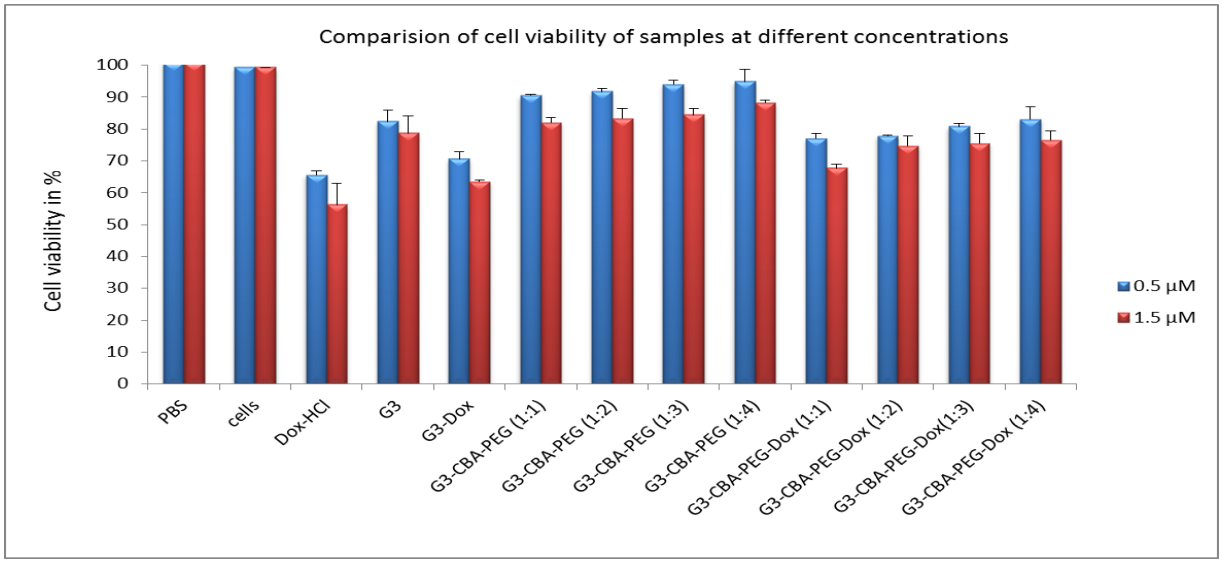

Figure 27 – Comparison of cell viability of CAL- 72 cells treated with 0.5 µM (blue) and 1.5 µM (red). The data are expressed as mean ± S.D.

3.6 Cellular uptake G3-CBA-PEG/DOX

The drug delivery systems should be effectively taken up by cells and be able to deliver the drug inside them. As DOX is a fluorescent molecule, its internalization by CAL-72 cells can be followed by fluorescence microscopy. Figure 28 shows the bright field and fluorescence microscope images of CAL-72 cells after 48 h in culture with DMEM (control), free DOX (1.5 μM), G3/DOX and G3-CBA-PEG/DOX with an equivalent amount of DOX (1.5 μM) diluted in the cell culture medium. The results show that a higher reddish intensity can be observed inside both cytosol and nucleus (especially in nucleus) after the cells were treated with the G3-CBA-PEG/DOX (G3/CBA is 1/4) for 48 h, compared to free DOX and the corresponding G3/DOX experiments. This higher DOX accumulation and enhanced anticancer activity may be attributed to the higher cell uptake of the G3-CBA-PEG/DOX nanoclusters and the improved DOX release intracellularly (probably due to reducible intracellular environments) (*92*), as well as to an acid-facilitated DOX release from the endo-lysosomal compartments to the nucleus. The above results indicate that the G3-CBA-PEG/DOX nanoclusters are able to effectively deliver DOX inside cancer cells.

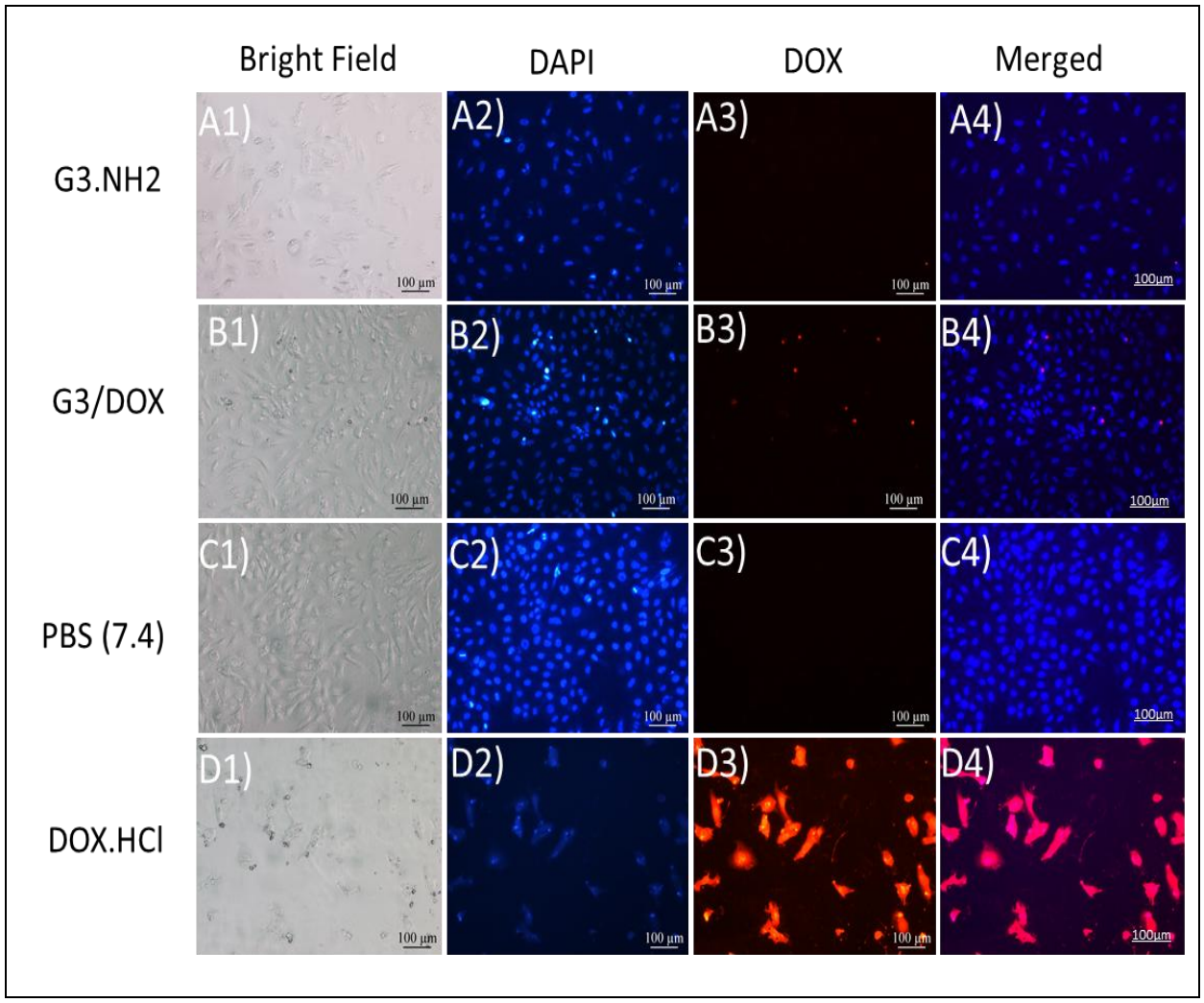
Bright Field
DAPI
DOX
Merged
G3.NH2
G3/DOX
PBS (7.4)
DOX.HCl
A1)
A2)
A3)
A4)
B1)
B2)
B3)
B4)
C1)
C2)
C3)
C4)
D1)
D2)
D3)
D4)
100 µm
100µm

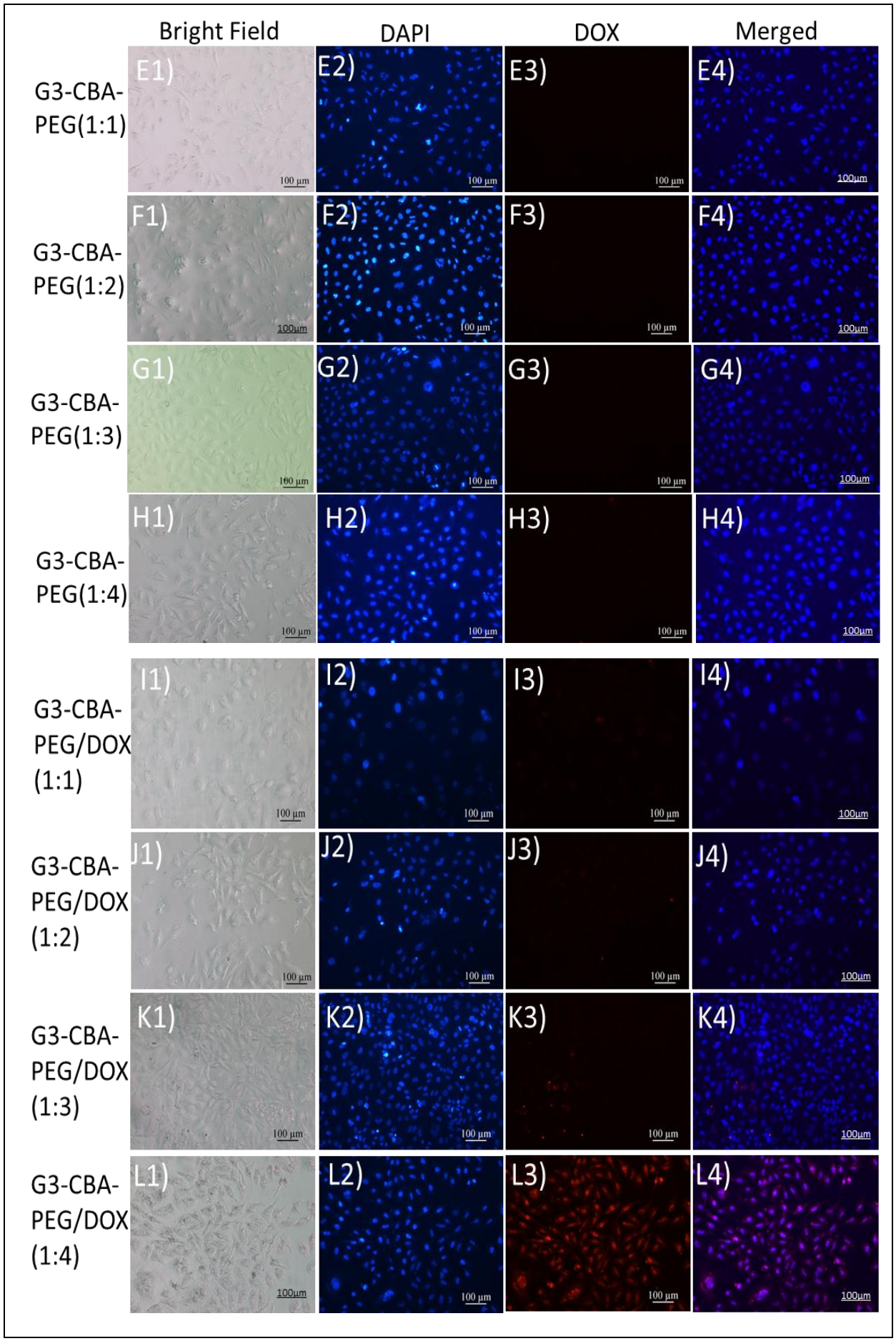
Bright Field
DAPI
DOX
Merged
G3-CBA-PEG(1:1)
E1)
E2)
E3)
E4)
G3-CBA-PEG(1:2)
F1)
F2)
F3)
F4)
G3-CBA-PEG(1:3)
G1)
G2)
G3)
G4)
G3-CBA-PEG(1:4)
H1)
H2)
H3)
H4)
G3-CBA-PEG/DOX (1:1)
I1)
I2)
I3)
I4)
G3-CBA-PEG/DOX (1:2)
J1)
J2)
J3)
J4)
G3-CBA-PEG/DOX (1:3)
K1)
K2)
K3)
K4)
G3-CBA-PEG/DOX (1:4)
L1)
L2)
L3)
L4)
100 µm

Figure 28 – Fluorescence microscopy images of CAL-72 cells, treated with G3-PAMAM for 48 hours (A), G3/DOX (B), PBS (pH 7.4) (C), DOX.HCl (D), G3-CBA-PEG (1:1) (E), G3-CBA-PEG (1:2) (F), G3-CBA-PEG (1:3) (G), G3-CBA-PEG (1:4) (H), G3-CBA-PEG/DOX (1:1) (I), G3-CBA-PEG/DOX (1:2) (J), G3-CBA-PEG/DOX (1:3) (K), G3-CBA-PEG/DOX (1:4) (L). In all cases, the DOX concentration was kept at 1.5 μM. For each panel, the images from left to right show bright field (series 1), blue fluorescence channel detecting the DAPI dye (series 2), red fluorescence channel detecting DOX (series 3), and merged images of blue fluorescence and red fluorescence channel (series 4). All the images were collected under similar instrumental conditions.

Summary

In this work, redox-sensitive G3-CBA-PEG dendrimer nanoclusters were synthesised by *in situ* crosslinking of low generation G3 dendrimers using CBA, followed by conjugation with mPEG-COOH. These nanoclusters were successfully encapsulated with DOX. The formed G3-CBA-PEG/DOX nanocomplexes were stable and displayed acid-accelerated drug release behaviour in tumor-mimic microenvironments and enhanced drug release property under intracellular reducible conditions. These merits, together with their enhanced biocompatibility, indicate that the G3-CBA-PEG/DOX nanocomplexes are able to effectively deliver DOX inside cancer cells. This work gives a new insight for the rational design of an optimal degradable platform for the intracellular delivery of therapeutic agents.

REFERENCES:

1. Yin, Q.; Shen, J. N.; Zhang, Z. W.; Yu, H. J.; Li, Y. P. Redox-responsive core cross-linked micelles based on cypate and cisplatin prodrugs-conjugated block copolymers for synergistic photothermal–chemotherapy of cancer. *Adv. Drug. Deliver. Rev*. **2013**, *65*, 1699 – 1715.
2. Oliveira, J. M.; Salgado, A. J.; Sousa, N.; Mano, J. F.; Reis, R. L. Dendrimers and derivatives as a potential therapeutic tool in regenerative medicine strategies—A review *Prog. Polym. Sci*. **2010**, *35*, 1163 – 1194.
3. Wang, Y.; Cao, X. Y.; Guo, R.; Shen, M. W.; Zhang, M. G.; Zhu, M. F.; Shi, X. Dendrimer-functionalized electrospun cellulose acetate nanofibers for targeted cancer cell capture applications. *Polym. Chem*. **2011**, *2*, 1754 – 1760.
4. Ertürka, A. S.; Tülüa, M.; Bozdoğana, A. E.; Paralib, T.; Microwave assisted synthesis of jeffamine cored PAMAM dendrimers. *J. Eur. Polym.* **2014,** *52*, 218- 226.
5. Fig. 1 www.nanosq.21c.osakafuu.ac.jp/ttsl_lab/c_kojima/e_kojima_research1.html Accessed at10.10.2014.
6. Prabal, K. M.; Tahir, C.; Guofeng, W.; William, A.G. Structure of PAMAM dendrimers: Generations 1 through 11. *Macromolecules.* **2004**, *37*, 6236 – 6254.
7. Tomalia, D.A.; Baker, H.; Dewald, J.; Hall, M.; Kallos, G.; Martin, S. et al. A new class of polymers: starburst-dendritic macromolecules. *Polym*. **1985**, *17*, 117–132.
8. Bosman, A. W.; Janssen, H. M.; Meijer, E. W. About Dendrimers: Structure, Physical Properties, and Applications. *Chem. Rev*. **1999**, *99*, 1665 – 1688.
9. Fischer, M.; Vögtle, F. Dendrimers. From design to application—a progress report, *Angew. Chem. Int. Ed. Engl.* **1999**, *38*, 884 – 905.
10. Dendrimers, *Topics Curr. Chem., Springer-Verlag, Heidelberg*. **1998,** *197*.
11. Dendrimers II - Architecture, Nanostructure and Supramolecular Chemistry, *Topics Curr. Chem., Springer-Verlag, Heidelberg.* **2000,** *210*.
12. Dendrimers III - Design, Dimension, Function, *Topics Curr. Chem., Spriner-Verlag, Heidelberg.* **2001**, *212*.

13. Dendrimers IV - Metal Coordination, Self-Assembly, Catalysis, *Topics Curr. Chem. Springer-Verlag, Heidelberg.* **2001,** *217*.

14. Dendrimers V, Topics *Curr. Chem. Springer-Verlag, Heidelberg*. **2003,** *228***.**

15. Tomalia, D.A.; Frechet, J.M.J.. Discovery of Dendrimer and Dendritic polymers: A brief Historical Perspective. *J.Polym.sci*: *Part A: Polym chem*. **2002**, *40*, 2719 – 2728.

16. Buhleier, E.; Wehner, W.; Vogtle, F. "Cascade"- and "Nonskid-Chain-like" syntheses of molecular cavity topologies. *Synthesis*, **1978**, *2*, 155–158.

17. Tomalia, D.A.; Majoros, I. Dendrimeric supramolecular and supramacromolecular assemblies, in: A. Ciferri (Ed.), *Supramol. Polym.* **2000**, 359 – 435.

18. Denkewalter, R.G.; Kolc, J.; Lukasavage, W.J. Macromolecular Highly Branched Homogeneous Compound. **1983**, U.S. Patent 4,410,688.

19. De Brabander-van den Berg E.M.M.; Meijer E.W. Poly (propylene imine) dendrimers: large-scale synthesis by heterogeneously catalysed hydrogenations. *Angew. Chem. Int. Ed*. **1993**, *32*, 1308–1311.

20. Wörner, C; Mülhaupt, R. Polynitrile- and polyamine-functional poly (trimethylene imine) dendrimers. *Angew. Chem. Int. Ed.* **1993**, *32*, 1306–1308.

21. Hawker, C.J.; Frechet, J.M.J. Preparation of polymers with controlled molecular architecture. A new convergent approach to dendritic macromolecules. *J. Am. Chem. Soc*. **1990**, *112*, 7638 – 7639.

22. Miller T.M.; Neenan T.X. Convergent synthesis of monodisperse dendrimers based upon 1,3,5-trisubstituted benzenes. *Chem Mater*. **1990**, *2*, 346–349.

23. Xu, Z.; Moore, J.S. Rapid construction of large-size phenylacetylene dendrimers up to 12.5 nanometers in molecular diameter. *Angew. Chem. Int. Ed.* **1993**, *32*, 1354–1357.

24. Xu, Z.; Moore, J.S. Synthesis and characterization of a high molecular weight stiff dendrimer. *Angew. Chem. Int. Ed*. **1993**, *32*, 246–248.

25. Franc, G.; Kakkar, A. K. Diels–Alder "Click" Chemistry in Designing Dendritic *Macromolecules.* **2009**, *15*, 5630 – 5639.

26. Franc, G.; Kakkar, A. K. Dendrimer design using Cu^{I}-catalyzed alkyne–azide ''click-chemistry''. *Chem. Commun.* **2008**, *15*, 5267–5276.

27. Yamagata, M.; Kawano, T.; Shiba, K.; Mori, T.; Katayama, Y.; Niidome, T. Structural advantage of dendritic poly(l-lysine) for gene delivery into cells. *Bioorg. Med. Chem*. **2007**, *15*, 526 – 532.

28. Volcke, C.; Pirotton, S.; Grandfils, C.; Humbert, C.; Thiry, P.A.; Ydens, I. et al. Influence of DNA condensation state on transfection efficiency in DNA/polymer complexes: an AFM and DLS comparative study. *Biotechnol*. **2006**, *125*, 11–21.

29. Gómez-Valadés, A.G.; Molas, M.; Vidal-Alabró, A.; Bermúdez, J.; Bartrons, R.; Perales, J.C. Copolymers of poly-l-lysine with serine and tryptophan form stable DNA vectors: implications for receptor-mediated gene transfer. *J. Control. Release*. **2005**, *102*, 277–291.

30. Barbara, K.; Maria, B. Dendrimers: properties and applications. *Acta. Biochim. pol.* **2001,** *48*,199 – 208.

31. Fréchet, J.M.J. Functional polymers and dendrimers: Reactivity, molecular architecture, and interfacial energy. *Science.* **1994**, *263*, 1710 –1715.

32. Jansen, J.F.G.A.; de Brabander-van den Berg, E.M.M.; Meijer, E.W. Encapsulation of guest molecules into a dendritic box. *Science.* **1994**, *266*, 1226 –1229.

33. Jansen, J.F.G.A.; Meijer, E.W. The dendritic box: Shape-selective liberation of encapsulatedguests. *J. Am. Chem. Soc*. **1995**, *117*, 4417– 4418.

34. Roberts, J.C.; Bhalgat, M.K; Zera, R.T. Preliminary biological evaluation of polyaminoamine (PAMAM) Starburst^{TM} dendrimers. *J. Biomed. Material. Res*. **1996**, *30*, 53 – 65.

35. Malik, N.; Wiwattanapatapee, R.; Klopsch, R.; Lorenz, K.; Frey, H.; Weener, J.W.; Meijer, E.W.; Paulus, W.; Duncan, R. Dendrimers: Relationship between structure and biocompatibility invitro, and preliminary studies on the bio distribution of ^{125}I-labelled polyamidoamine dendrimers in vivo. *J. Controlled. Release*. **2000**, *65*, 133 –148.

36. Mourey, T.H.; Turner, S.R.; Rubenstein, M.; Fréchet, J.M.J.; Hawker, C.J.; Wooley, K.L. Unique behaviour of dendritic macromolecules: Intrinsic viscosity of polyether dendrimers. *Macromolecules*. **1992**, *25*, 2401–2406.

37. Antoni, P.; Hed, Y.; Nordberg, A.; Nyström, D.; von Holst, H.; Hult, A.; Malkoch, M. Bifunctional dendrimers: from robust synthesis and accelerated one-pot post

functionalization strategy to potential applications. *Angew. Chem. Int. Ed. Engl*. **2009**, *48*, 2126 – 2130.

38. James, R.; Mc Elhanon.; Dominic, V. Mc. toward Chiral Polyhydroxylated Dendrimers. Preparation and Chiroptical Properties. *J. Org. Chem*. **2000**, *65*, 3525 – 3529.
39. Catherine, O. L.; Fréchet, J.M.J. Incorporation of Functional Guest Molecules into an Internally Functionalizable Dendrimer through Olefin Metathesis. *Macromolecules*. **2005**, *38*, 6276 – 6284.
40. Nanjwade, B. K.; Bechra, H.M.; Derkar, G.K.; Manvi, F.V.; Nanjwade, V.K. Dendrimers: emerging polymers for drug-delivery systems. *Eur. J. Pharm. Sci*. **2009**, *38*, 185 – 96.
41. Ballauf, M. Dendrimers III: Design, dimension, function. *Topics Curr. Chem*. **2001**, *212*, 177 – 178.
42. Ballauf, M.; Likos, C.L. Dendrimers in solution: insight from theory and simulation. *Angew. Chem. Int. Ed. Engl*. **2004**, *43*, 2998– 3020.
43. Boas, U.; Christensen, J.B.; Heegaard, P.M.H. Dendrimers in medicine and biotechnology. *J. Mater.Chem.* **2006**, *16*, 3785 – 3798.
44. Newkome, G.R.; Moorefield, C.N.; Vögtle, F. Dendrimers and dendrons: concepts, syntheses, applications. *Wiley-VCH, Weinheim*, Germany. **2001**.
45. Newkome, G.R.; Moorefield, C.N.; Baker, G.R. Alkane cascade polymers processing micellar topology: micellanoic acid derivatives. *Angew. Chem. Int. Ed.* **1991**, *30*, 1178– 1180.
46. Tomalia, D.A.; Naylor, A.M.; Goddard, W.A.; Starburst dendrimers: molecular-level control of size, shape, surface chemistry, topology, and flexibility from atoms to macroscopic matter. *Angew. Chem. Int. Ed.* **1990**, *29*, 138 – 141.
47. Bethany, H. C & EN, Washington. *Chem. Eng. News*. **2005**, *83*, 30 – 36.
48. Tomalia, D.A.; Baker, H.; Dewald, J.; Hall, M..; Kallos, G.; Martin, S.; Roeck, J.; Ryder, J.; Smith, P. Dendritic macromolecules: synthesis of starburst dendrimers. *Macromolecules*. **1986**, *19*, 2466 – 2468.
49. Van Duijvenbode, R. C.; Borkovec, M.; Koper, G. J. M. Acidbase properties of poly (propylene imine) dendrimers. *Polymer*. **1998**, *39*, 2657.
50. Prabal K. M.; Tahir. C.; Shiang-Tai, L.; William A. G. III. Effect of solvent and pH on the structure of PAMAM Dendrimers. *Macromolecules.* **2005**, *38*, 979-991.

51. Maingi, V.; Mattaparthi, V. S. K.; Prabal, K. M. PAMAM dendrimer–drug interactions: effect of pH on the binding and release pattern. *J. Phys. Chem. B.* **2012**, *116*, 4370–4376.
52. Sönke, S.; Tomalia, D.A. Dendrimers in biomedical applications reflections on the field. *Adv. Drug. Del. Rev*. **2012**, *64*, 102–115.
53. Woo-Dong, J.; Kamruzzaman Selim, K.M.; Chi-Hwa, L.; Inn-Kyu, K. Bioinspired application of dendrimers: From bio-mimicry to biomedical applications. *Prog. Polym. Sci.* **2009**, *34*, 1–23.
54. Szymański, P.; Markowicz, M.; Mikiciuk-Olasik, E.; Nanotechnology in pharmaceutical and biomedical applications: dendrimers. *Nano.* **2011**, *6*, 509 –539.
55. Maha, N.; Mohammad, N.; D'Emanuele, A.; Abdelbary, E. PAMAM dendrimers as aerosol drug nanocarriers for pulmonary delivery via nebulization. *Int. J. Pharmaceutics*. **2014**, *461*, 242–250.
56. Magdalena, M.P.; Emilia, Ł.; Maciej, C.; Marlena, B.; Elżbieta M.O.; Joanna, S. Studies towards biocompatibility of PAMAM dendrimers – Overall hemostasis potential and integrity of the human aortic endothelial barrier. *Int. J. Pharmaceutics.* **2014** *473*, 158–169.
57. Perisé-Barriosa, A.J.; Jiménezb J.L.; Domínguez-Sotoe, A.; Matac J. D.L.; Corbíe A L.; Gomez R.; Muñoz-Fernandeza, M. Á. Carbosilane dendrimers as gene delivery agents for the treatment of HIV infection. *J. Controlled Release*. **2014**, *184*, 51–57.
58. Kui, L.; Caixia, L.; Gang, W.; Yu, N.; Bin, H.; Yao, W.; Zhongwei G. Peptide dendrimers as efficient and biocompatible gene delivery vectors: Synthesis and in vitro characterization. *J. Controlled Release*. **2011**, *155*, 77–87.
59. Kui, L.; Caixia, L.; Li, L.; Wenchuan, S.; Gang, W.; Zhongwei, G. Arginine functionalized peptide dendrimers as potential gene delivery vehicles. *Biomaterials*, **2012**, *33*, 4917– 4927.
60. Hay, B.P.; Werner, E.J.; Raymond, K.N. Estimating the number of bound waters in Gd(III) complexes revisited. Improved methods for the prediction of q-values, *Bioconjug. Chem*. **2004**, *15*, 1496 –1502.
61. Brambilla, D.; Nicolas, J.; Le Droumaguet, B. Design of fluorescently tagged poly(Alkyl Cyanoacrylate) nanoparticles for human brain endothelial cell imaging. *Chem. Commun*. **2010**, *46*, 2602 – 2604.

62. Doubrovin, M.; Serganova, I.; Mayer-Kuckuk, P.; Ponomarev, V.; Blasberg, R.G.; Multimodality in vivo molecular-genetic imaging, *Bioconjug. Chem.* **2004,** *15*, 1376 – 1388.

63. Medley, C.D.; Smith, J.E.; Tang, Z. Gold nanoparticle-based colorimetric assay for the direct detection of cancerous cells. *Anal. Chem*. **2008**, *80*, 1067 – 1072.

64. Wang, Y.; Guo, R.; Cao, X. Encapsulation of 2-methoxyestradiol within multifunctional Poly(Amidoamine) dendrimers for targeted cancer therapy. *Biomaterials.* **2011**, *32*, 3322 – 3329.

65. Panyam, J.; Labhasetwar, V. Biodegradable nanoparticles for drug and gene delivery to cells and tissue. *Adv. Drug Deliv. Rev*. **2003**, *55*, 329 – 347.

66. Kui, L.; Gang, L.; Wenchuan, S.; Qiaoying, W.; Gang, W.; Bin, H.; Hua, A.; Qiyong, G.; Bin, S.; Zhongwei, G. Gadolinium-labeled peptide dendrimers with controlled structures as potential magnetic resonance imaging contrast agents. *Biomaterials*. **2011**, *32*, 7951–7960.

67. Fernandes Edson, G. R.; Vieira Nirton, C. S.; de Queiroz Alvaro, A. A.; Guimaraes Francisco, E. G.; Zucolotto, Valtencir. Immobilization of poly(propylene imine) dendrimer/nickel phthalocyanine as nanostructured multilayer films to be used as gate membranes for SEGFET pH sensors. *J. Phys. Chem*. **2010,** *114*, 6478–6483.

68. Campos, B.; Algarra, M.; Esteves Da Silva, J. C. G. Fluorescent properties of a hybrid cadmium sulfide-dendrimer nanocomposite and its quenching with nitromethane. *J. Fluorescence*, **2010**, *20*, 143 –151.

69. Kono, K.; Liu, M.; Fréchet, J.M.J. Design of dendritic macromolecules containing folate or methotrexate residues. *Bioconjug. Chem*. **1999,** *10*, 1115–1121.

70. Quintana, A.; Raczka, E.; Piehler, L.; Lee, I.; Myc, A.; Majoros, I.; Patri, A.K.; Thomas, T.; Mule, J.; Baker, J.R. Design and function of a dendrimer-based therapeutic nanodevice targeted to tumor cells through the folate receptor, *Pharm. Res*. **2002**, *19,* 1310–1316.

71. Ross, J.F.; Chaudhuri, P.K.; Ratnam, M. Differential regulation of folate receptor isoforms in normal and malignant tissues in vivo and established cell lines. Physiologic and clinical implications, *Cancer*. **1994**, *73*, 2432–2443.

72. Shukla, S.; Wu, G.; Chatterjee, M.; Yang, W.; Sekido, M.; Diop, L.A.; Muller, R.; Sudimack, J.J.; Lee, R.J.; Barth, R.F.; Tjarks, W. Synthesis and biological evaluation of folate receptor-targeted boronated PAMAM dendrimers as potential agents for neutron capture therapy. *Bioconjug. Chem*. **2003**, *14*, 158–167.

73. Boas, U.; Heegaard, P.M.H.; Dendrimers in drug research. *Chem. Soc. Rev*. **2004**, *33*, 43–63.

74. Kubasiak, L.A.; Tomalia, D.A. Cationic dendrimers as gene transfection vectors, in:M.M. Amiji (Ed.), Polymeric Gene Delivery: Principles and Applications, *CRC Press, Boca Raton*, FL, **2004**, 133–157.

75. Liu, M.; Fréchet, J.M.J. Designing dendrimers for drug delivery, *Pharm. Sci. Technol. Today*, **1999,** *2*, 393–401.

76. Battah, S.H.; Chee, C.E.; Nakanishi, H.; Gerscher, S.; MacRobert, A.J.; Edwards, C. Synthesis and biological studies of 5-aminolevulinic acid-containing dendrimers for photodynamic therapy. *Bioconjug. Chem.* **2001**, *12*, 980–988.

77. Paul, A.; Hackbarth, S.; Molich, A.; Luban, C.; Oelckers, S.; Bohm, F.; Roder, B. Comparative study of the photosensitization of Jurkat cells in vitro by pheophorbide a and a pheophorbide a–diaminobutane poly(propylene imine) dendrimer complex. *Laser Phys*. **2003**, *13*, 22–29.

78. Bourne, N.; Stanberry, L.R.; Kern, E.R.; Holan, G.; Matthews, B.; Bernstein, D.I.; Dendrimers, a new class of candidate topical microbicides with activity against herpes simplex virus infection. *Antimicrob. Agents Chemother.* **2000,** *44*, 2471–2474.

79. Vauthier, C.; Dubernet, C.; Chauvierre, C. Drug Delivery to Resistant Tumors: The Potential of Poly(Alkyl cyanoacrylate) Nanoparticles. *J. Control. Release.* **2003**, *93*, 151-160.

80. Yih, T.; Al-Fandi, M. Engineered Nanoparticles as Precise Drug Delivery Systems. *J. Cell. Biochem*. **2006**, *97*, 1184-1190.

81. Malik, N.; Evagorou, E.G.; Duncan, R. Dendrimer–platinate: a novel approach to cancer chemotherapy. *Anticancer Drugs.* **1999**, *10*, 767–776.

82. Sonke, S.; Chauhan, A.S. Dendrimers for enhanced drug solubilization. *Nanomedicine*, **2008**, *3*, 679 – 702

83. Maeda, H.; Seymour, L. W.; Miyamoto, Y. Conjugates of anticancer agents and polymers: advantages of macromolecular therapeutics in vivo. *Bioconjugate Chem*. **1992**, *3*, 351–362.
84. Maeda, H.; Wu, J.; Sawa, T.; Matsumura, Y.; Hori, K. Tumor vascular permeability and the EPR effect in macromolecular therapeutics. *J. Controlled Release*. **2000**, *65*, 271–284.
85. Morgan M.T.; Nakanishi Y.; Kroll D.J.; Griset A.P.; Carnahan M.A.; Wathier M.; Oberlies N.H.; Manikumar G.; Wani M.C.; Grinstaff M.W. Dendrimer-encapsulated camptothecins. *Am. Assoc. Canc. Research*. **2006**, *66*, 11913–11921.
86. Tekade R.K.; Dutta T.; Gajbhiye V.; Jain N.K. Exploring dendrimer towards dual drug delivery. *J. Microencapsulation.* **2009**, *26*, 287–296.
87. Anne-Marie, C.; Cedric-Oliver, T. Dendrimers for drug delivery. *J. Mater. Chem. B.* **2014**, *2*, 4055–4066.
88. Roberts, J.C.; Bhalgat, M.K.; Zera, R.T. Preliminary biological evaluation of polyamidoamine (PAMAM) starbust dendrimers. *J. Biomed. Mater. Research*. **1996**, *30*, 53 – 65.
89. Saltzman, W. M.; Torchilin, V. P. "Drug delivery systems". Access Science. McGraw-Hill Companies. Bertrand N, Leroux JC. **2011.** http://accessscience.com/content/Drug%20delivery%20systems/757275. Accessed at 15.10.2014
90. Varun, A. Nanotechnology Drug Delivery Systems: An Insight, **2012**. http://trialx.com/curetalk/2012/10/nanotechnology-drug-delivery-systems-an-insight. Accessed at 14.10.2014.
91. Tran, P.A.; Zhang, L., Webster, T.J. Carbon nanofibers and carbon nanotubes in regenerative medicine. *Adv. Drug Deliv. Rev.* **2009**, *61*, 1097–1114.
92. Safari, J.; Zarnegar, Z. Advanced drug delivery systems: Nanotechnology of health design. A review. *J. Saudi. Chem. Soc.* **2014**, *18*, 85-99.
93. Maeda, H.; Wu, J.; Sawa T. Tumor vascular permeability and the EPR effect in macromolecular therapeutics: A Review. *J. Control Release.* **2000**, *65*, 271 – 284.
94. Patri, A.K.; Kukowska Latallo, J.F.; Baker Jr, J.R. Targeted drug delivery with dendrimers: Comparison of the release kinetics of covalently conjugated drug and non-covalent drug inclusion complex. *Adv. Drug. Deliv. Rev.* **2005**, *57*, 2203 – 2214.

95. Amir, R. J.; Pessah, N.; Shamis, M.; Shabat, D. Self-Immolative Dendrimers. *Angew. Chem., Int. Ed.* **2003**, *42*, 4494 – 4499.

96. Zimmerman, S. C.; Zharov, I.; Wendland, M. S.; Rakow, N. A.; Suslick, K. S. Molecular imprinting inside dendrimers. *J. Am. Chem. Soc.* **2003**, *125*, 13504 – 13518.

97. Muzafarov, A. M.; Golly, M.; Moeller, M. Degradable hyperbranched Poly(bis(undecenyloxy)methylsilane)s. *Macromolecules.* **1995**, *28*, 8444 – 8446.

98. Aulenta, F.; Drew, M. G. B.; Foster, A.; Hayes, W.; Rannard, S.; Thornthwaite, D. W.; Youngs, T. G. A. Fragrance release from the surface of branched poly(amide)s. *Molecules.* **2005**, *10*, 81 – 97.

99. Kohman, R. E.; Zimmerman, S. C. Degradable dendrimers divergently synthesized via click chemistry. *Chem. Commun.* **2009**, 794 – 796.

100. Wei, H.; Kou, H.; Shi, W.; Yuan, H.; Chen, Y. Photopolymerization kinetics of dendritic poly(ether-amide)s. *Polymer*. **2001**, *42*, 6741– 6746.

101. Carnahan, M. A.; Middleton, C.; Kim, J.; Kim, T.; Grinstaff, M. W. Hybrid dendritic-linear polyester-ethers for in situ photopolymerization. *J. Am. Chem. Soc.* **2002**, *124*, 5291 – 5293.

102. Carnahan, M. A.; Grinstaff, M. Synthesis and characterization of poly(glycerol-succinic acid) dendrimers. *Macromolecules.* **2001**, *34*, 7648 – 7655.

103. Luman, N. R.; Smeds, K. A.; Grinstaff, M. The convergent synthesis of poly(glycerol-succinic acid) dendritic macromolecules. *Chem. Eur. J.* **2003**, *9*, 5618 – 5626.

104. Boury, B.; Corriu, R. J. P.; Nuñez, R. Hybrid xerogels from dendrimers and arborols. *Chem. Mater*. **1998**, *10*, 1795 – 1804.

105. Dvornic, P. R.; Li, J.; de Leuze-Jallouli, A. M.; Reeves, S. D.; Owen, M. J. Nanostructured dendrimer-based networks with hydrophilic polyamidoamine and hydrophobic organosilicon domains. *Macromolecules*. **2002**, *35*, 9323 – 9333.

106. Kohli, N.; Dvornic, P. R.; Kaganove, S. N.; Worden, R. M.; Lee, I. Nanostructured crosslinkable micropatterns by amphiphilic dendrimer stamping. *Macromol. Rapid Comm.* **2004**, *25*, 935 – 941.

107. Chao, L.; Zhiyuan, Z.; Martin, C. L.; Xulin, J.; Wim, E. H.; Jan, F.; Johan, F.J. E. Linear poly(amido amine)s with secondary and tertiary amino groups and variable

amounts of disulfide linkages: Synthesis and in vitro gene transfer properties. *J. Controlled Release*. **2006**, *116*, 130 –137

108. Brocchini, S.; Godwin, A.; Balan, S.; Choi, J.; Zloh, M.; Shaunak, S. Disulfide- bridge based PEGylation of proteins. *Adv. Drug. Deliv. Rev.* **2008**, *60*, 3–12.
109. Olivier, J. C. Drug transport to brain with targeted nanoparticles. *Neuro Rx.* **2005,** *2*, 108 – 119
110. Torchilin, V. P. Recent advances with liposomes as pharmaceutical carriers, *Nat. Rev. Drug. Discov*. **2005**, *4*, 145 – 160.
111. Nawalany, K.; Kozik, B.; Kepczynski, M.; Zapotoczny S.; Kumorek, M.; Nowakowska, M.; Jachimska, B. Properties of polyethylene glycol supported tetra aryporphyrin in aqueous solution and its interaction with liposomal membranes. *J. Phys. Chem. B.* **2008,** *112*, 12231 – 12239.
112. Veronese, F. M.; Pasut, G. PEGylation for improving the effectiveness of therapeutic biomolecules. *Drugs Today*. **2009**, *45*, 687– 695.
113. Dinc, C. O.; Kibarer, G.; Guner, A. Solubility profiles of poly(ethylene glycol)/solvent systems. II. Comparison of thermodynamic parameters from viscosity measurements, *J. Appl. Polym. Sci*. **2010,** *117*, 1100 – 1119.
114. Chiou, W. L.; Riegelman S. Pharmaceutical applications of solid dispersion systems, *J. Pharm. Sci.* **1971**, *60*, 1281 – 1302.
115. Serajuddin, A. T. M. Solid dispersion of poorly water-soluble drugs: early promises, subsequent problems, and recent breakthroughs, *J. Pharm. Sci.* **1999**, *88* 1058 – 1066.
116. Leuner, J. D. Improving drug solubility for oral delivery using solid dispersions, *Eur. J. Pharm. Biopharm*. **2000**, *50*, 47 – 60.
117. Xianjun, Y.; Yuqing, Z.; Changyi, C.; Qizhi, Y.; Min, L. Targeted drug delivery in pancreatic cancer. *Biochim. Biophys. Acta- Rev. on Cancer.* **2010**, *1805*, 97-104.
118. Guiottoa, A.; Canevaria M.; Michela S.; Orsolinib P.M.; Francesco M. Anchimeric assistance effect on regioselective hydrolysis of branched PEGs: a mechanistic investigation. *Bioorg. Med. Chem.* **2004**, 12, 5031 – 5037.
119. Bailon, A.; Palleroni, C.A.; Schaffer, C.L.; Spence, W.J.; Fung, J.E.; Porter, G.K.; Ehrlich, W.; Pan, Z.X.; Modi, M.W. Rational design of a potent, long-lasting form of interferon: a 40 k.Da branched polyethylene glycol-conjugated interferon alpha-2a for the treatment of hepatitis C. *Bioconjugate Chem.* **2001**, 12, 195 – 202.
120. Duncan, R. The dawning era of polymer therapeutics. *Nat. Rev*. **2003**, *2*, 347 – 360.

121. Kojima Lab, Dept. Applied Chemistry, Grad. Sch. Engineering .Osaka Prefecture University. www.chem.osakafu u.ac.jp/ohka/kojima_lab/e_kojima_research2.html. Accessed in17.10.2014.

122. Sheehan, J.C.; Preston, J.; Cruickshank, P.A. A rapid synthesis of oligonucleotide derivatives without isolation of intermediates. *J. Am. Chem. Soc.***1965**, *87*, 2492-2493.

123. Greg, T.H. Bio conjugate techniques. *Acad. Press. London.* **1996,** *1*, 170 – 171.

124. Roberts, M.J.; Bentley, M.D.; Harris, J.M. Chemistry for peptide and protein PEGylation. *Adv. Drug. Deliv. Rev.* **2002**, *54*, 4.59 – 476.

125. Kawai, F. Microbial degradation of polyethers. *Appl. microbial. biotechnol.* **2002**, *58*, 30 – 38.

126. Jonathan H. B.; Chao, L.; James, Y.; Won, J. K.; Katherine S.; Blevins, Johan F. J.; Engbersen, J.F.; Sung W.K. Mixtures of poly(triethylenetetramine/cystamine bisacrylamide) and poly(triethylenetetramine/cystamine bisacrylamide)-g-polyethylene glycol for improved gene delivery. *Bioconjugate Chem.* **2010**, *21*, 1753 – 1761.

127. Tongbing, S.; Yong, J.; Rui, Q.; Shaojun, P.; Baozhu, F.; Oxidation responsive mono-cleavable amphiphilic di-block polymer micelles labeled with a single diselenide. *Polym. Chem.* **2013**, *4*, 4017 – 4023.

128. Chichong, L.; Lok, R.B.; Hong, Y. J.; Seong H. P.; Kyu Y. C. Carboxyl–polyethylene glycol–phosphoric acid: a ligand for highly stabilized iron oxide nanoparticles. *J. Mater. Chem.* **2012**, *22*, 19806-19811.

129. Chunmei, G.; Mingzhu, L.; Shaoyu, L.; Xinjie, Z.; Yuanmou, C.; Synthesis and self-assembly of PAMAM/PAA Janus dendrimers. *Mater. Res. Express.* **2014**, *1*, 1–12.

130. Yin, W.; Xueyan, C.; Rui, G.; Mingwu, S.; Mengen, Z.; Meifang, Z.; Xiangyang S.; Targeted delivery of doxorubicin into cancer cells using a folic acid–dendrimer conjugate. *Polym. Chem.* **2011**, *2*, 1754–1760.

131. Molavia, O.; Xiao-Bing, X.; Douglas, D.; Knetemand, N.; Nagatae, S.; Pastan. I.; Chug, Q.; Lavasanifarc A.; Laia. Anti-CD30 antibody conjugated liposomal doxorubicin with significantly improved therapeutic efficacy against anaplastic large cell lymphoma. *Biomaterials.* **2013**, *34, 8718–8725.*

ANNEX

ANNEX I – ^{1}H NMR spectra with integration and identifications of peaks.

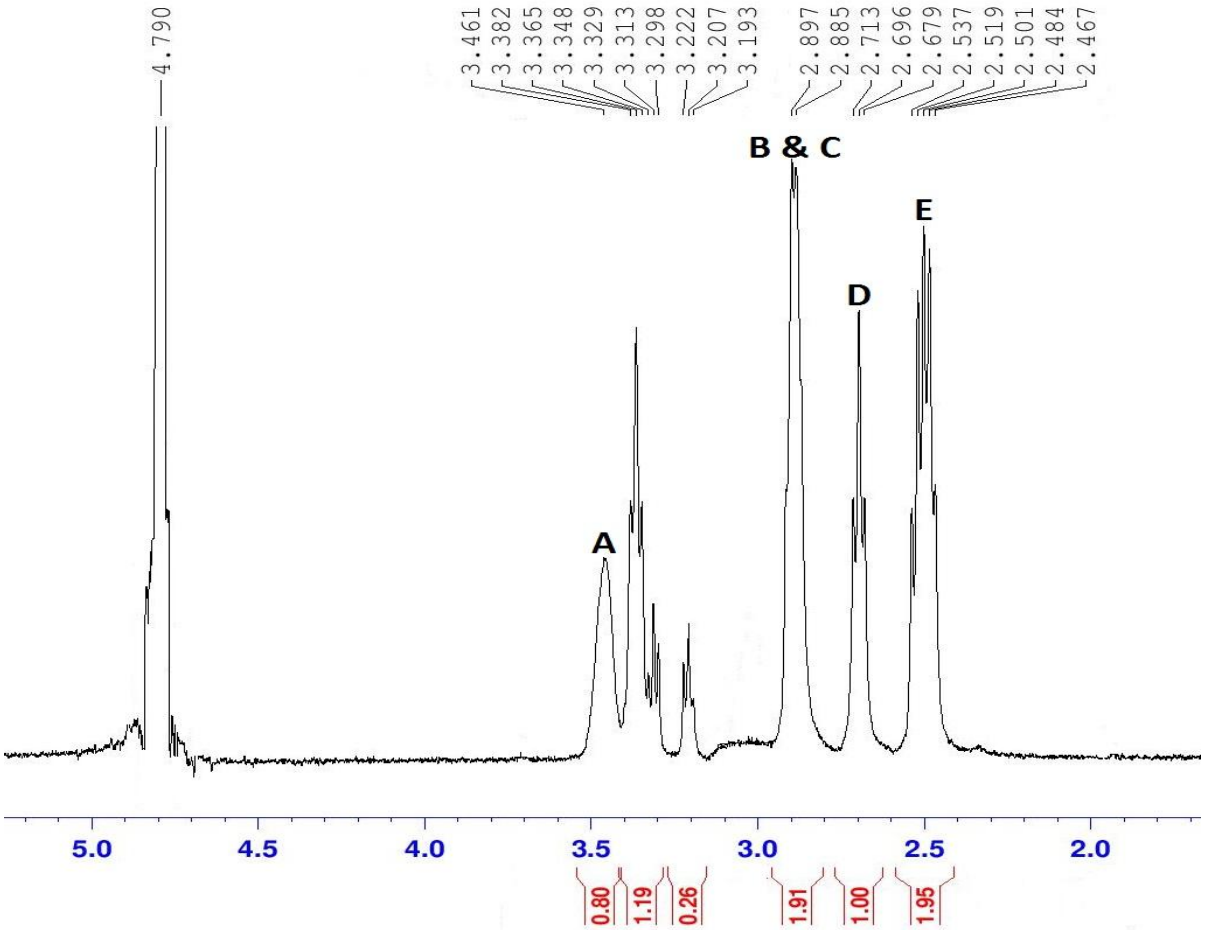

Figure 29 – ^{1}H NMR spectrum of G3-PAMAM dendrimer in D_2O with integration and peak identifications.

A = $CONHCH_2$; **B** = $CONHCH_2CH_2NH_2$; **C** = NCH_2CH_2CONH; **D** = $CH_2CH_2NR_2$; **E** = CH_2CONH. (*76*).

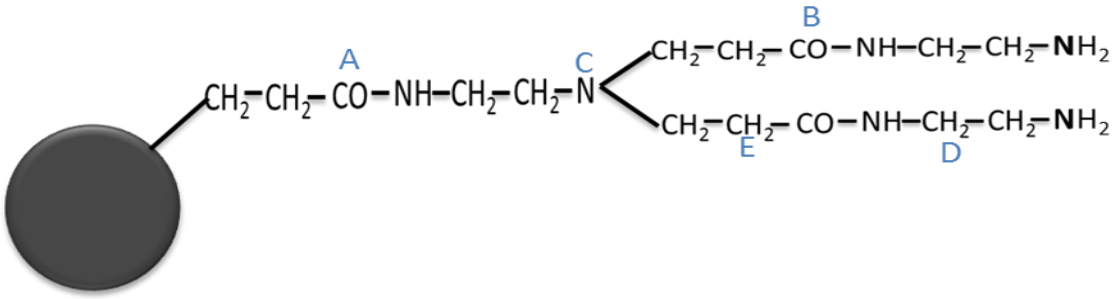

G3-PAMAM dendrimer with terminal groups, the black ball represents the core structure of the dendrimer.

ANNEX II – FTIR spectra with identifications of peaks.

Preparation of Pellets for FTIR analysis

G3-PAMAM dendrimer was 5 mg was mixed with 20 mg of KBr and was finely grinded until the mixture has the consistency of fine flour. The mixture was then transferred into the cylindrical bore and evenly distributed. The mixture was subjected to a hydraulic pressure of 10 tons, after 1 minute the pressure was released. The sample was found to be evenly distributed and the disk was translucent. Then the sample disk was analysed using FTIR spectroscopy.

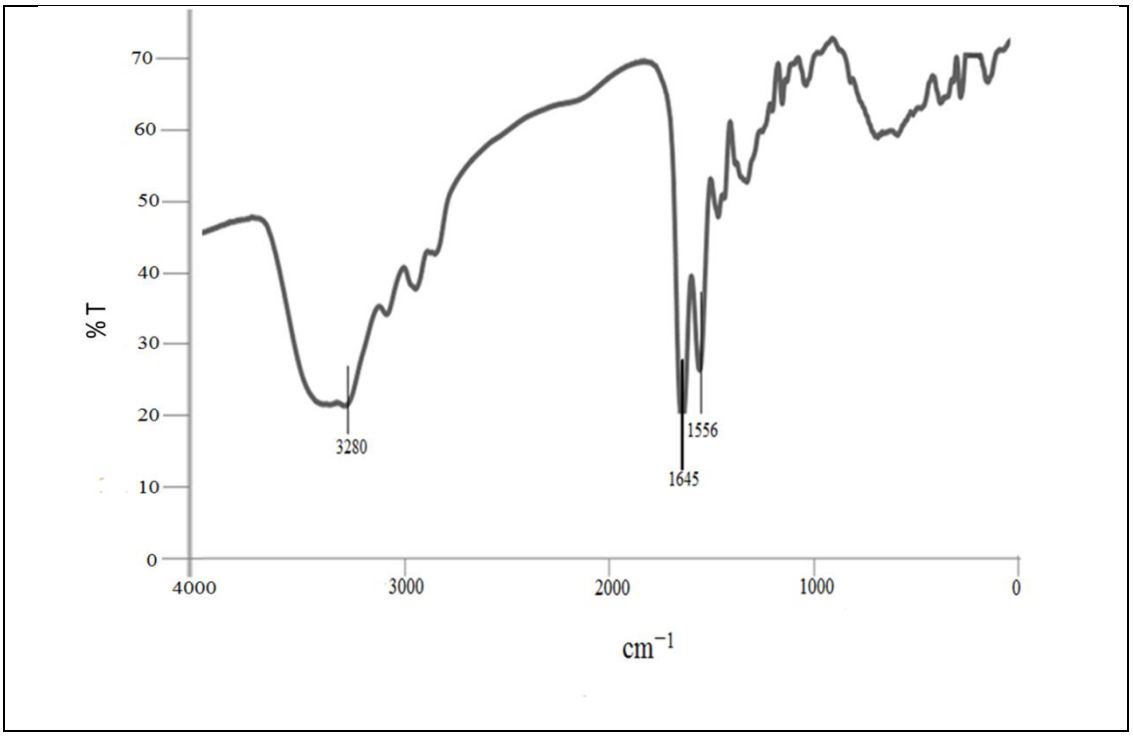

Figure 30 – FTIR spectrum of G3.NH_2 PAMAM dendrimer with identification of peaks.

Characteristic peaks of G3-PAMAM dendrimer

N-H band at 3280 cm^{-1}

C=O band at 1645 cm^{-1} and

N-H bending at 1556 cm^{-1}

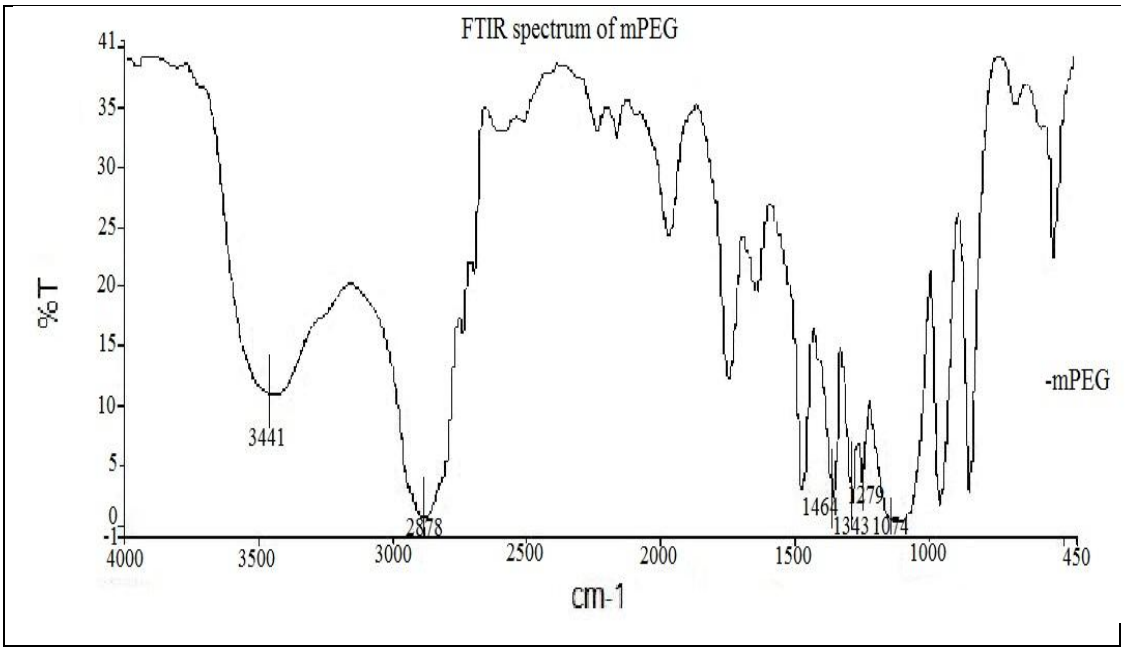

Figure 31 – FTIR spectrum of mPEG with identification of peaks.

Characteristic peaks of mPEG observed in FTIR spectrum

O-H Stretching: 3441 cm^{-1}

C-H stretching: 2878 cm^{-1}

C-H extended Stretching: 1464 and 1343 cm^{-1}

O-H AND C-O-H stretching: 1279 and 1074 cm^{-1}

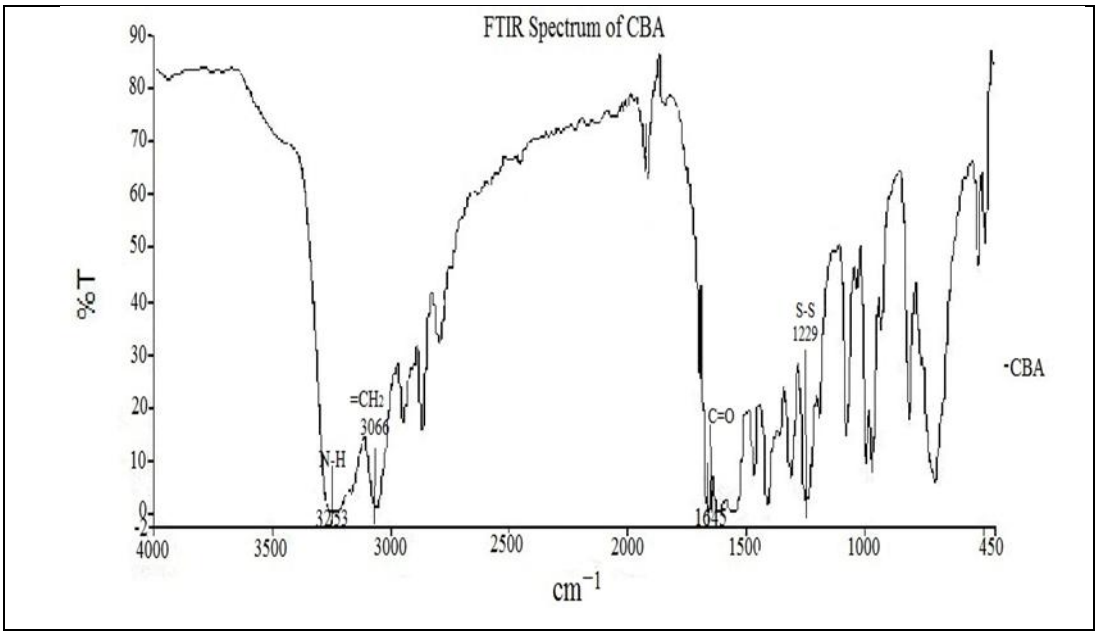

Figure 32 – FTIR spectrum of CBA with identification of peaks.

The characteristic peaks observed in the FTIR spectrum of CBA

S-S band at 1229 cm^{-1},

N-H band at 3253 cm^{-1},

C=O band at 1645 $cm^{-1}$and

$=CH_2$ at 3066 cm^{-1}.

ANNEX III – Study of stability of particles.

Samples without DOX G3-CBA-PEG							
G3:CBA	**day 1**	**day 2**	**day 3**	**day 4**	**day 5**	**day 6**	**day 7**
01:01	172.8 ± 1.21	172.91 ± 1.45	172.5 ± 0.9	172.68 ± 1.24	172.65 ± 1.37	172.84 ± 1.89	172.75 ± 1.54
01:02	175.1 ± 0.54	175.21 ± 1.67	175.69 ± 1.24	175.43 ± 1.05	175.58 ± 1.21	175.37 ± 1.4	175.25 ± 1.2
01:03	285.4 ± 3.5	285.3 ± 6.4	285.57 ± 5.2	285.9 ± 4.8	285.85 ± 3.28	285.38 ± 4.1	285.44 ± 5.06
01:04	411 ± 8.05	411.4 ± 3.51	411.21 ± 4.08	411.49 ± 6.2	411.32 ± 5.9	411.15 ± 7.9	411.12 ± 6.8
Samples with DOX G3-CBA-PEG/DOX							
G3:CBA	**day 1**	**day 2**	**day 3**	**day 4**	**day 5**	**day 6**	**day 7**
01:01	190.1 ± 2.87	190.85 ± 3.23	190.72 ± 5.71	190.6 ± 4.83	190.43 ± 6.21	190.21 ± 4.12	189.8 ± 7.65
01:02	323.8 ± 1.59	323.5 ± 2.66	323.1 ± 2.4	322.7 ± 3.09	322.5 ± 4.8	322.3 ± 3.78	322.1 ± 4.28
01:03	369.9 ± 5.44	369.7 ± 4.32	368.8 ± 6.84	368.2 ± 3.87	368.02 ± 5.61	367.92 ± 4.87	367.77 ± 6.38
01:04	446.7 ± 7.52	446.3 ± 8.65	446.1 ± 7.94	445.8 ± 8.21	445.5 ± 8.79	445.2 ± 9.53	444.21 ± 10.87

ANNEX IV – Study of drug release kinetics.

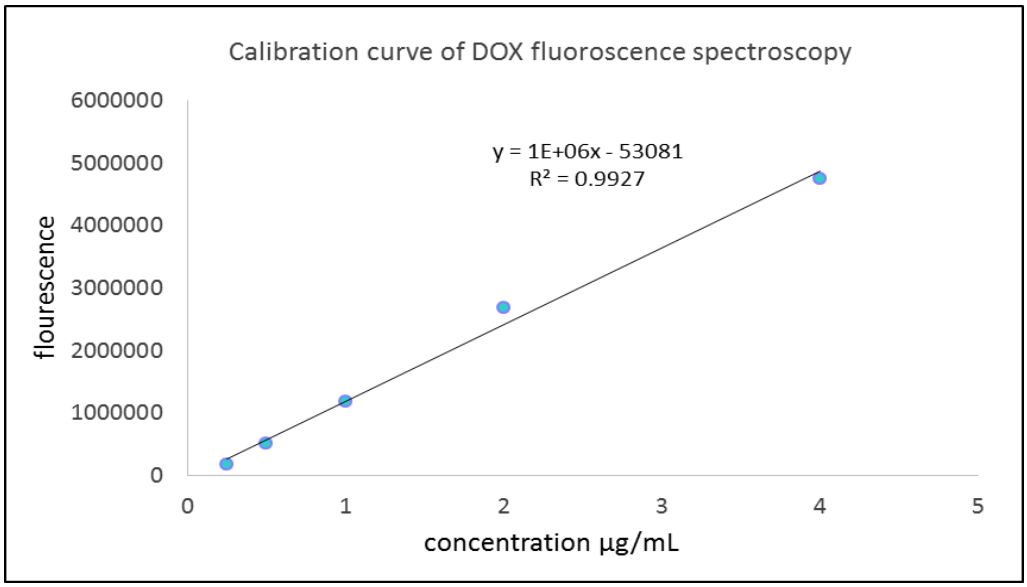

Figure 33 – Calibration curve of DOX by fluorescence spectroscopy.

For measuring the standard curve of DOX by fluorescence spectroscopy, DOX was prepared in concentrations of 0.25, 0.5, 1, 2, and 4µg/mL. The samples were taken in a micro plate reader (100 µL each sample) and the fluorescence was measured at 590 nm.

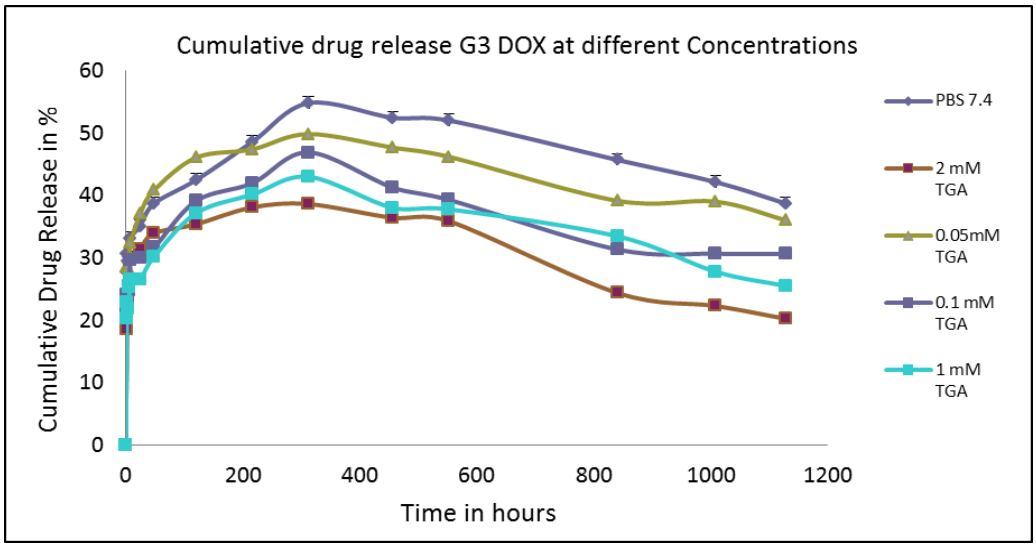

Figure 34 – Cumulative drug release of G3/DOX at different concentrations of TGA compared with release profile at PBS (pH 7.4).

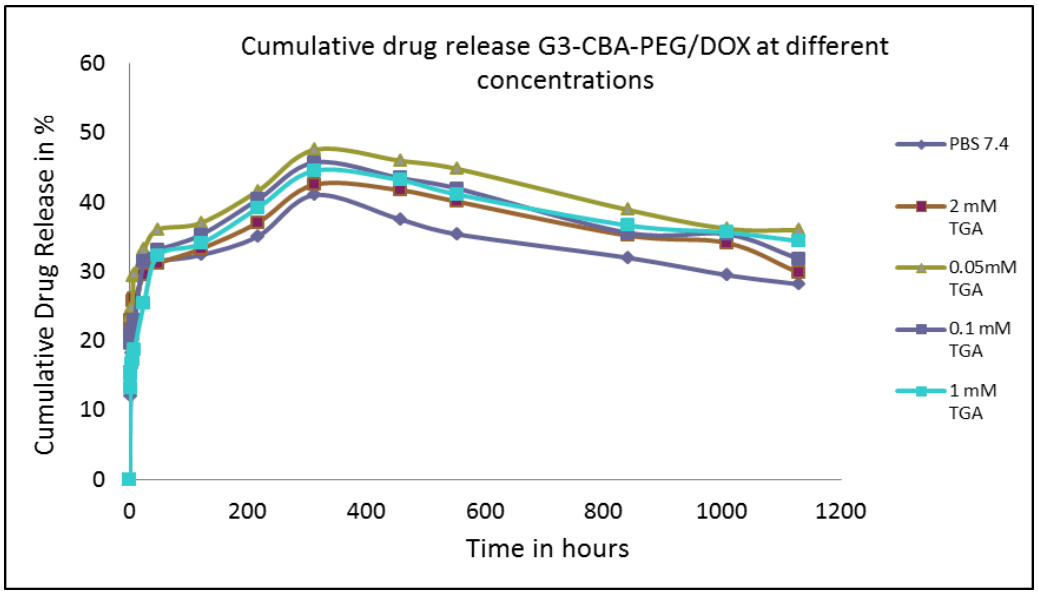

Figure 35 – Cumulative drug release of G3-CBA-PEG/DOX (G3:CBA 1:1) at different concentrations of TGA compared with release profile at PBS (pH 7.4).

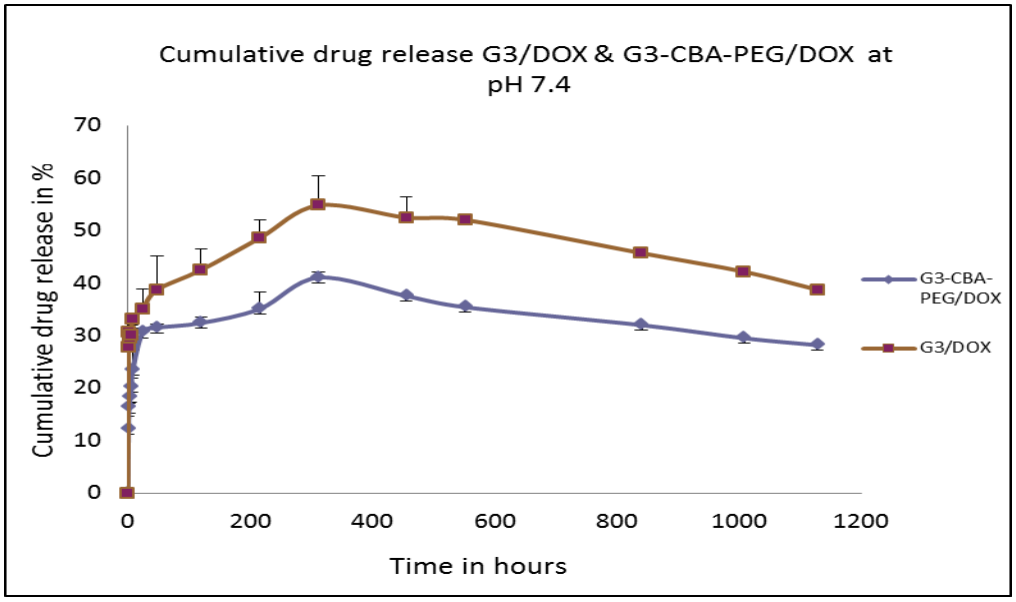

Figure 36 – Comparison of cumulative drug release of G3/DOX and G3-CBA-PEG/DOX (G3:CBA 1:1) at PBS (pH 7.4).

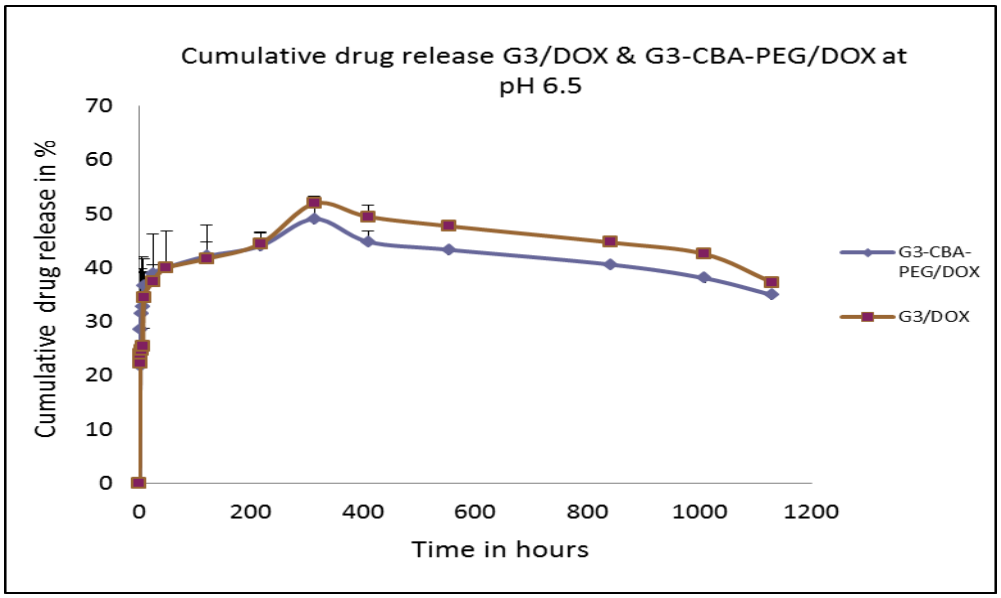

Figure 37 – Comparison of cumulative drug release of G3/DOX and G3-CBA-PEG/DOX (G3:CBA 1:1) at PBS (pH 6.5).

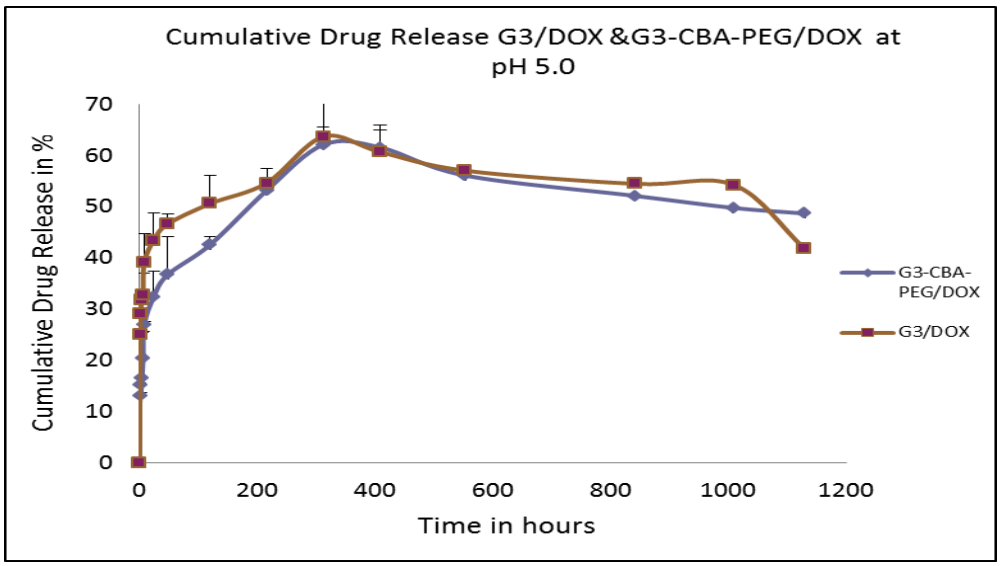

Figure 38 – Comparison of cumulative drug release of G3/DOX and G3-CBA-PEG/DOX (G3:CBA 1:1) at PBS (pH 5.0).

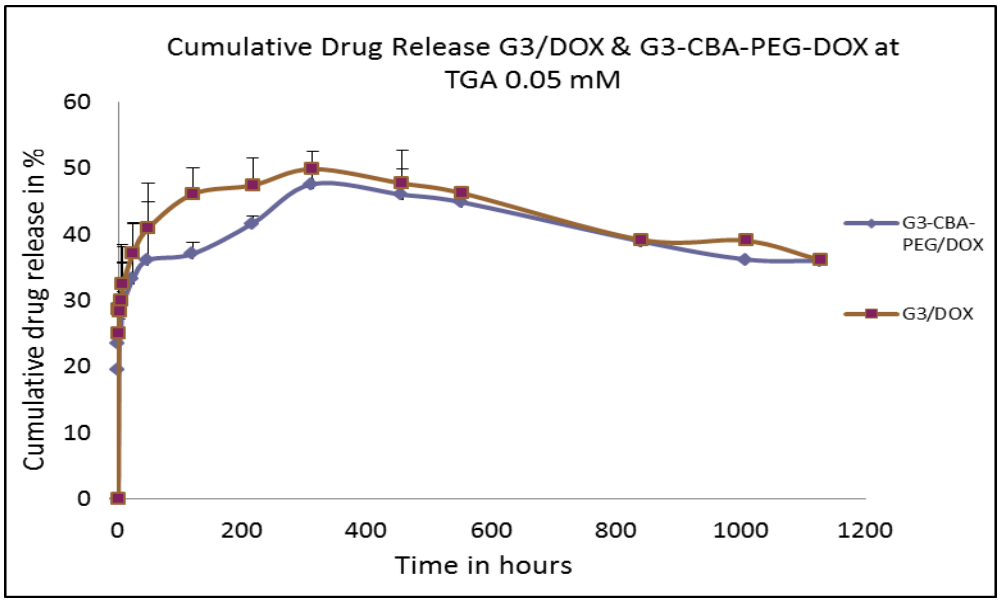

Figure 39 – Comparison of cumulative drug release of G3/DOX and G3-CBA-PEG/DOX (G3:CBA 1:1) at TGA 0.05 mM.

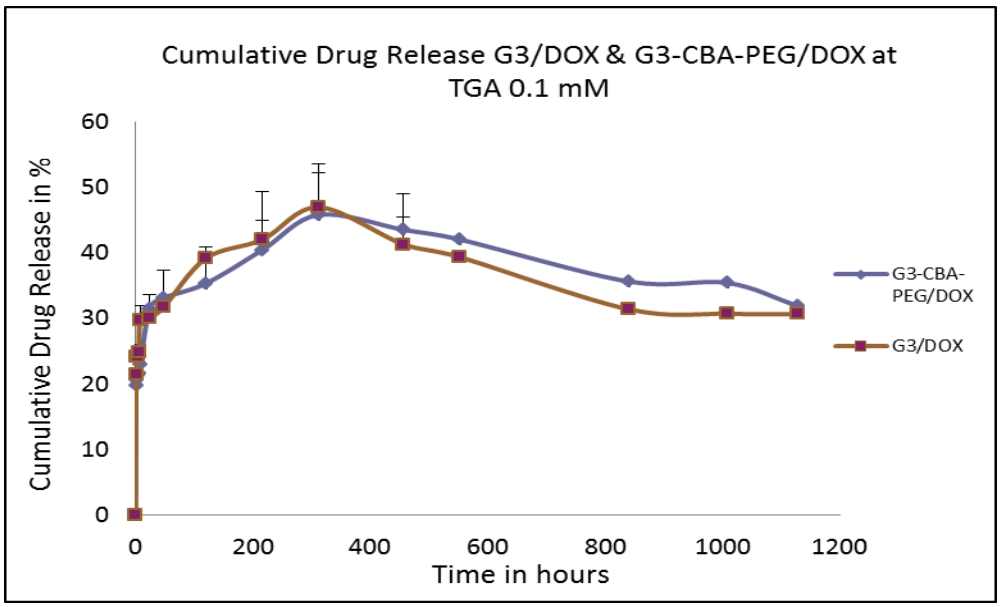

Figure 40 – Comparison of cumulative drug release of G3/DOX and G3-CBA-PEG/DOX (G3:CBA 1:1) at TGA 0.1 mM.

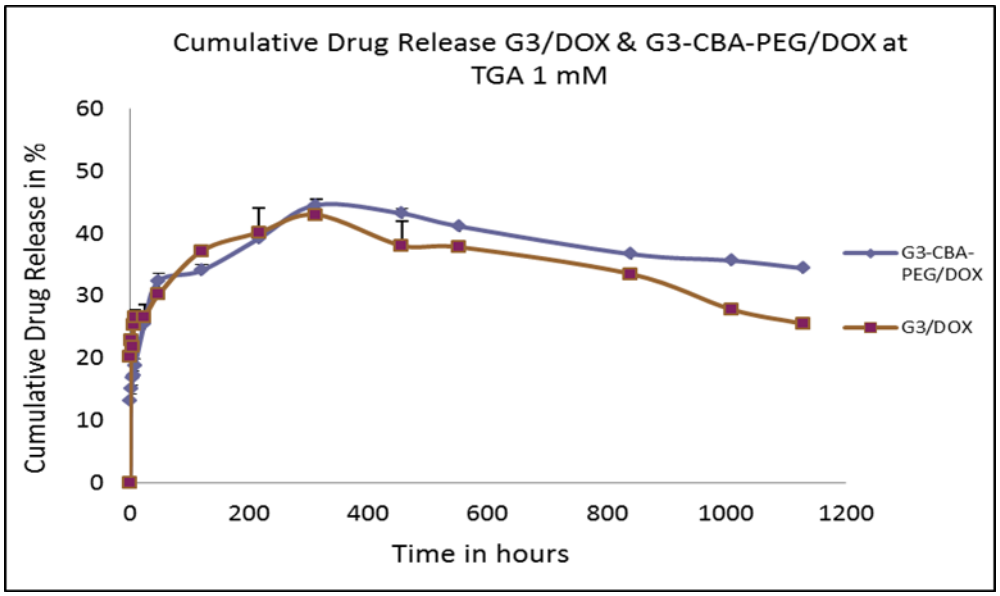

Figure 41 – Comparison of cumulative drug release of G3/DOX and G3-CBA-PEG/DOX (G3:CBA 1:1) at TGA 1 mM.

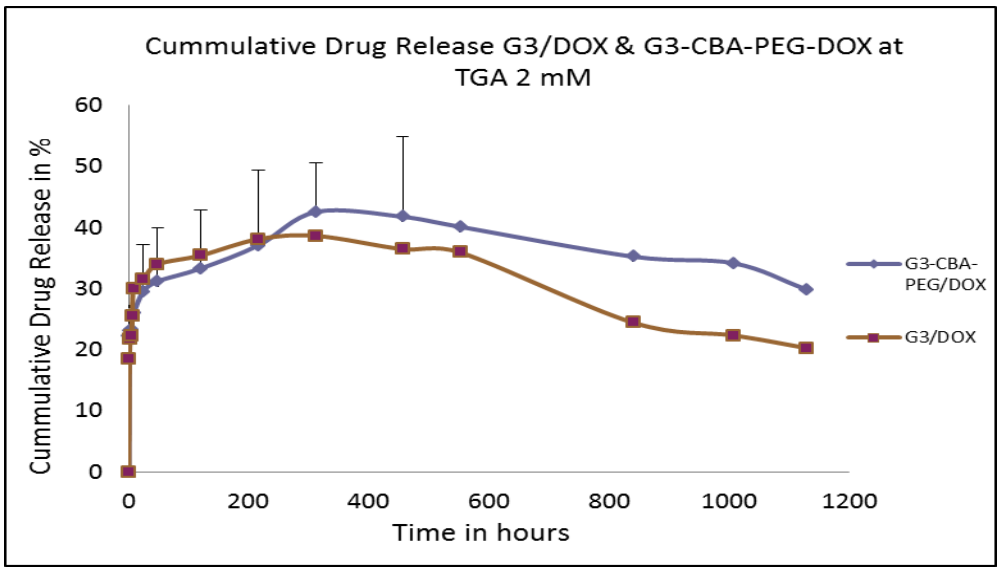

Figure 42 – Comparison of cumulative drug release of G3/DOX and G3-CBA-PEG/DOX (G3:CBA 1:1) at TGA 2 mM.

ANNEX V – Cytotoxic studies of CAL-72 cell line with different concentrations of DOX.

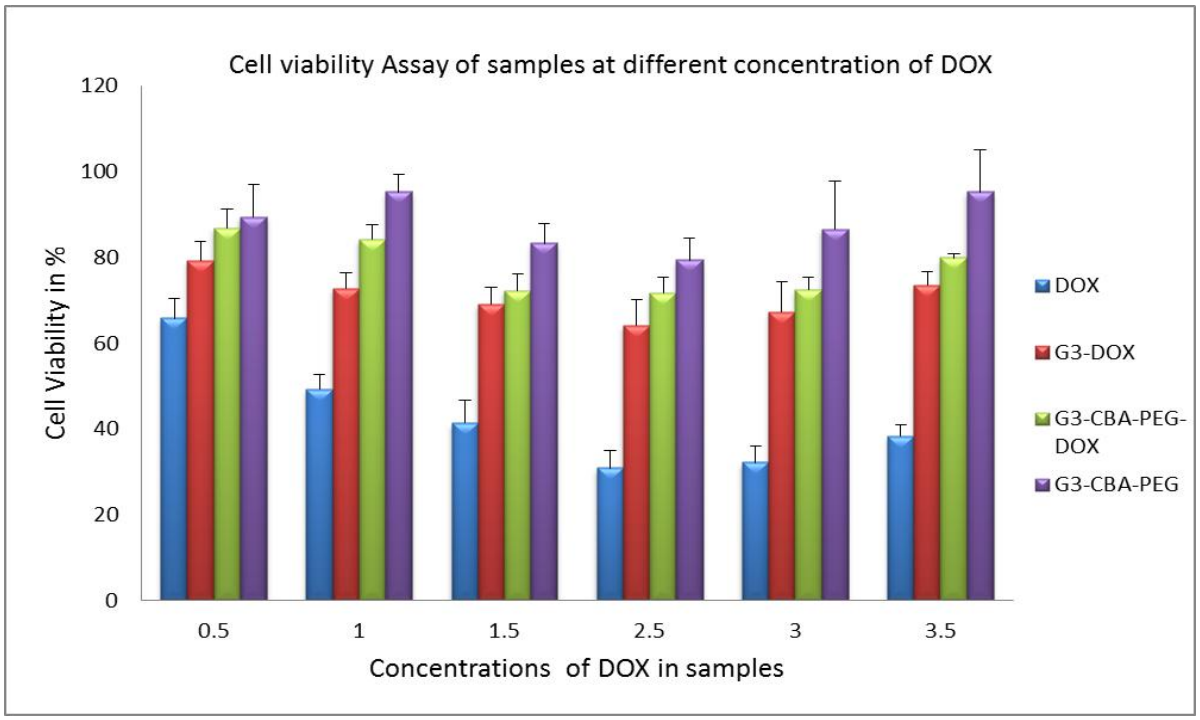

Figure 43 – Comparison of cell viability of DOX.HCl (Blue column), G3/DOX (Red column), G3-CBA-PEG/DOX (G3:CBA 1:1), (Green column) and G3-CBA-PEG (G3:CBA 1:1) (Violet column) at different concentrations.

Note that cells treated with PBS 7.4 and DMEM medium are not shown in the Figure and are reported in the Figure 22 and 23. The concentration of the DOX is kept constant for all the samples at specified concentration except the sample without DOX.

UNIVERSIDADE da MADEIRA

CQM CENTRO DE QUÍMICA DA MADEIRA

Molecular Materials ®
RESEARCH GROUP
MADEIRA ISLAND - PORTUGAL

FCT Fundação para a Ciência e a Tecnologia
MINISTÉRIO DA EDUCAÇÃO E CIÊNCIA

Governo da República Portuguesa

União Europeia

Região Autónoma da Madeira